Article type:

Submitted version – Preprint

Identification of the First PPARα/γ Dual Agonist Able to Bind to Canonical and Alternate Sites of PPARγ and to Inhibit its Cdk5-Mediated Phosphorylation

Antonio Laghezza,[1] Luca Piemontese,[1] Carmen Cerchia,[2] Roberta Montanari,[3] Davide Capelli,[3] Marco Giudici,[4] Maurizio Crestani,[4] Paolo Tortorella,[1] Franck Peiretti,[5] Giorgio Pochetti,[3] Antonio Lavecchia,[2] Fulvio Loiodice*[1]

[1] *Dipartimento Farmacia-Scienze del Farmaco, Università degli Studi di Bari "Aldo Moro", via Orabona 4, 70125 Bari, Italy*

[2] *Dipartimento di Farmacia, "Drug Discovery" Laboratory, Università degli Studi di Napoli "Federico II", via D. Montesano 49, 80131 Napoli, Italy*

[3] *Istituto di Cristallografia, Consiglio Nazionale delle Ricerche, Montelibretti, 00015 Monterotondo Stazione, Roma, Italy*

[4] *Dipartimento di Scienze Farmacologiche e Biomolecolari, Università degli Studi di Milano, via Balzaretti 9, 20133 Milano, Italy*

[5] *Aix Marseille Université, INSERM 1263, INRA 1260, C2VN, 13005 Marseille, France*

Abstract

A new series of derivatives of the PPARα/γ dual agonist **1** allowed to identify the ligand (*S*)-**6** as a potent partial agonist of both PPARα and γ subtypes. X-ray studies in PPARγ revealed two different binding modes of (*S*)-**6** to canonical site. However, (*S*)-**6** was also able to bind an alternate site as demonstrated by transactivation assay in the presence of a canonical PPARγ antagonist and supported from docking experiments. This compound did not activate the PPARγ-dependent program of adipocyte differentiation inducing a very less severe lipid accumulation compared to rosiglitazone, but increased the insulin-stimulated glucose uptake in 3T3-L1 adipocytes. Finally, (*S*)-**6** inhibited the Cdk5-mediated phosphorylation of PPARγ at serine 273 that is currently considered the mechanism by which some PPARγ partial agonists exert antidiabetic effects similar to thiazolidinediones, without showing their typical side effects. This is the first PPARα/γ dual agonist reported to show this inhibitory effect representing the potential lead of a new class of drugs for treatment of dyslipidemic type 2 diabetes.

INTRODUCTION

Type 2 diabetes mellitus (T2DM) strikes nearly 300 million people worldwide and represents a major cause of morbidity and mortality.[1] This chronic metabolic disorder results in a combination of dyslipidemia, glucose intolerance, and inflammation. Peroxisome proliferator-activated receptors (PPARs) are ligand-activated transcription factors that play a key role in the regulation of a large number of genes whose products are directly or indirectly involved in glucose homeostasis and lipid metabolism. For this reason, they have been considered suitable targets for the treatment of metabolic disorders.

There are three distinct PPAR subtypes, PPARα, PPARγ, and PPARδ, with different tissue distributions and physiological functions. PPARα is important for the uptake and oxidation of fatty acids and lipoprotein metabolism and is the molecular target of fibrates, a class of drugs that lower plasma triglycerides and increase HDL cholesterol levels in humans.[2-4] Furthermore, PPARα-agonists can increase the stability of atherosclerotic plaques, reduce the risk of atherothrombosis, and reduce hepatic fat accumulation leading to non-alcoholic steatohepatitis/fatty liver disease (NASH/NAFLD).[5] Fibrates are weak PPARα-agonists whose efficacy is partly limited by dose-dependent side effects. Commonly reported adverse events include elevations in markers for cardiovascular disease, renal disease, and liver dysfunction.[3,4,6] To address this problem, a new generation of more potent PPARα agonists with a lower potential for adverse effects is being developed. In some cases, a greater lipid-modifying efficacy associated with an improved safety/tolerability profile has been obtained.[7,8] Thiazolidinediones (TZDs), including rosiglitazone and pioglitazone, are the only clinically available agents controlling hyperglycemia by improving insulin resistance, which is regarded as hallmark and early etiologic basis for T2DM. TZDs have been demonstrated to behave as PPARγ full agonists, which activate PPARγ leading to a wide spectrum of genes expression changes involved in insulin sensitizing activity.[9] However, recent studies have demonstrated that the use of these compounds is associated with unwanted effects, such as weight gain, fluid retention, increased incidence of cardiovascular events, and bone

fractures.[10-13] Different strategies have been conceived to obtain compounds with good therapeutic potential, trying to avoid the known side effects.

In particular, PPARα/γ dual agonists represent a promising solution given that they exhibit the insulin sensitizing potential of PPARγ agonists along with the beneficial lipid modulating activities of PPARα agonists.[14] Dual-acting PPARα/γ agonists, therefore, could simultaneously correct insulin resistance and lipid imbalance, thereby overcoming the side effects of selective PPARγ agonists. In the past, several dual PPARα/γ agonists have been developed and evaluated[15-19] and recently, one such agent, saroglitazar, has been approved in India for the treatment of diabetic dyslipidemia and hypertriglyceridemia with type 2 diabetes not controlled by statin therapy.[20] Saroglitazar is predominantly a PPARα agonist, with modest PPARγ agonist actions. This is in contrast to previously developed dual PPARα/γ agonists, which had either predominantly PPARγ agonistic activity or similar agonistic activity on both PPARα and PPARγ receptors. In particular, an appropriate modulation of PPARγ activity appears the key challenge for the development of a dual agonist able to uncouple the adverse effects of the ligand from therapeutic effects. In this regard, recent observations indicate that the improved therapeutic profile of selective PPARγ modulators (SPPARγMs) compared to PPARγ full agonists is a consequence of peculiar ligand-receptor interactions resulting in a different structural conformation of the complex that gives rise to different PPAR transcriptional signatures.[21-26] Recently, studies from Choi et al.[21,22] have shown that cyclin-dependent kinase 5 (Cdk5)-mediated phosphorylation of PPARγ at serine 273 may be involved in the pathogenesis of insulin resistance. S273 phosphorylation leads to dysregulation of a large number of PPARγ target genes that are known to be associated with insulin sensitization. Inhibition of the S273-phosphorylation was thus proposed as a plausible mechanism by which anti-diabetic PPARγ partial agonists or modulators increase insulin sensitivity, without activating the full range of PPARγ target genes, and thereby avoiding known side effects such as fluid retention, bone fractures, and weight gain.

In our previous studies, we have reported the synthesis and biological activity of a number of

carboxylic acid derivatives showing an interesting dual activity toward PPARα and PPARγ receptors.[25-34] In particular, we identified the lead compound LT175 ((S)-**1**, Fig. 1), a dual PPARα/γ ligand with a partial agonism profile toward the γ subtype.[35] The X-ray structure of the complex with PPARγ showed that this compound interacts with the receptor in a newly identified hydrophobic region called "diphenyl pocket" inducing a conformation of the ligand binding domain (LBD) less favorable to the recruitment of coactivators required for full activation of PPARγ. This new interaction influences the expression of PPARγ target genes, leading to an improved therapeutic profile compared with rosiglitazone. In fact, (S)-**1** showed potent insulin-sensitizing effects with reduced adipogenic properties.[36] The corresponding R enantiomer of (S)-**1** ((R)-**1**, Fig. 1) is still active on PPARγ even though with lower potency and slightly reduced efficacy. Interestingly, the two stereoisomers occupy different regions of the receptor as shown from the X-ray structure of their complex with PPARγ-LBD (Fig. 1): (S)-**1** occupies a branch named "diphenyl pocket" between helices H11 and H3, whereas (R)-**1** accommodates in the region usually occupied by other known partial agonists, between helix H3 and the β-sheet.[35] With the aim to evaluate the effects resulting from the combination of both binding modes, we designed the two novel molecular scaffolds shown in Fig. 2: compound **2** originates from the fusion of the diphenyl systems of two molecules of (R,S)-**1**, whereas compound **3** derives from the fusion of the benzyl ring of one molecule of (R,S)-**1** with the diphenyl nucleus of a second molecule. For this compound a gradual structural simplification of the distal part of the molecule was also realized obtaining derivatives **4-6**. All the racemates of this series were evaluated for their PPARα/γ activity by the transactivation assay. For the most active compounds **3** and **6** we prepared all the corresponding stereoisomers to explore the influence of absolute configuration on receptor activation. (S)-**6** turned out to be the ligand with the most interesting pharmacological profile able to potently activate both PPARα and γ subtypes as a partial agonist. Further in vitro experiments confirmed that (S)-**6** is devoid of some of the known side effects of PPARγ full agonists, but significantly increased the insulin-stimulated glucose uptake. X-ray studies and docking experiments were performed on the complex PPARγ/(S)-

6 to gain more insights into the molecular mechanism of PPARγ activation and revealed different binding modes with both canonical and alternate sites. Finally, (*S*)-**6** was able to inhibit the Cdk5-mediated phosphorylation of PPARγ at serine 273. As far as we know, this ligand is the first PPARα/γ dual agonist reported to show this inhibitory effect. A compound with these properties is expected to exhibit the beneficial lipid modulating activities of PPARα agonists along with the insulin sensitizing potential of PPARγ agonists but without the typical side effects of selective PPARγ full agonists. Therefore, (*S*)-**6** may represent the potential lead of a new class of drugs with better pharmacological properties in the treatment of dyslipidemic type 2 diabetes.

CHEMISTRY

The synthesis of compound **2** is depicted in Scheme 1 and was carried out starting from the ethyl ester of racemic phenyllactic acid and 4,4'-diphenol, which were condensed, under Mitsunobu conditions, to obtain the diester intermediate **2b**. This two-step procedure ensured better yields compared to the single-step one utilizing a molar ratio 2:1 of the starting materials. The hydrolysis of **2b** allowed to obtain the desired acid. The synthesis of racemic compounds **3-5** is reported in scheme 2 and started from the ethyl esters of phenyllactic, 2-bromopropanoic or bromoacetic acids, respectively. These esters were alternatively reacted with 4-hydroxyphenylboronic acid pinacol ester, under Mitsunobu conditions, to give the ester intermediates **3a-5a**. These underwent Suzuki coupling by condensation with ethyl 2-(4-phenyl-phenoxy)-3-(4-bromophenyl)propanoate **6e** (see scheme 3) affording diesters **3b−5b**, which were hydrolyzed to the desired acids. The racemic acid **6** was prepared through the procedure represented in scheme 3. Diethyl 2-chloro-malonate was reacted with sodium 4-phenyl-phenate to give diester **6a** which was condensed with 4-bromo-benzylbromide in the presence of NaH affording **6b**. The subsequent Suzuki coupling of this intermediate with benzeneboronic acid gave the diester **6c** whose saponification and decarboxylation led to the target acid. Alternatively, **6b** was hydrolyzed and decarboxylated to **6d** which was transformed into the corresponding ethyl ester **6e** to be used as reported in scheme 2.

The synthesis of the four stereoisomers of compound **3** was carried out similarly to the corresponding racemate (see scheme 2) starting from the readily available (*S*)- or (*R*)-ethyl phenyllactates. The Mitsunobu reaction of these starting materials with 4-hydroxyphenylboronic acid pinacol ester occurred with inversion of configuration affording the esters (*R*)-**3a** and (*S*)-**3a**, respectively (scheme 4). These intermediates were condensed alternatively with (*S*)- or (*R*)-ethyl 2-(4-phenyl-phenoxy)-3-(4-iodophenyl)propanoate **6g** (see scheme 5) obtaining the four stereoisomers of **3b**, which were hydrolyzed to the corresponding optically active acids. Finally, (*R*)-**6** and (*S*)-**6** were prepared as depicted in scheme 5. The commercially available (*R*)- or (*S*)-4-iodo-phenylalanines were converted into the corresponding hydroxy-esters (*R*)-**6f** and (*S*)-**6f** through a procedure known to occur with retention of configuration.[37] These intermediates were condensed with 4-phenylphenol under Mitsunobu conditions affording compounds (*S*)-**6g** and (*R*)-**6g**, respectively, with inverted configuration. The Suzuki cross-coupling reaction with benzeneboronic acid and the final hydrolysis led to the target acids.

The diastereomeric (de) and/or enantiomeric excesses (ee) of all optically active isomers were determined by HPLC analysis on chiral stationary phase (see the Experimental Section).

RESULTS AND DISCUSSION

Compounds **2-6** were evaluated in vitro for their agonist activity toward the human PPARα (hPPARα) and PPARγ (hPPARγ) subtypes by employing GAL4-PPAR transactivation assay. For this purpose, GAL4-PPAR chimeric receptors were expressed in transiently transfected HepG2 cells according to a previously reported procedure.[27] In particular, the results obtained were compared with corresponding data for Wy-14,643 and rosiglitazone used as reference compounds in the PPARα and PPARγ transactivation assays, respectively. Maximum obtained fold induction with the reference agonist was defined as 100%. The activity of **2-6** was also compared with the lead compound (*S*)-**1**.

As a preliminary test, we evaluated the efficacy of racemates **2-6** on PPARα and PPARγ at

concentrations increasing up to 100 μM. As shown in Fig. 3, compound **2** was completely inactive, whereas **4** and **5** showed only a low activation of both subtypes. As a whole, only **3** and **6** showed a moderate activity and, for this reason, we prepared all the stereoisomers of these two compounds and determined their potency and efficacy (Table 1). Compared to (*S*)-**1** and reference compounds, the four stereoisomers of **3** exhibited lower activity in terms of efficacy and/or potency on PPARα and PPARγ with (R^I,R^{II})-**3** being completely inactive on the former. Both receptors displayed a significant stereoselectivity toward the four stereoisomers whose activity showed the following rank order: (S^I,S^{II}) > (S^I,R^{II}) > (R^I,S^{II}) > (R^I,R^{II}). With regard to compound **6**, the *S* enantiomer was more potent and effective than the *R* enantiomer on PPARα; however, both acted as partial agonists compared to (*S*)-**1** and reference compound. The behavior of these two enantiomers was slightly different on PPARγ; in fact, they were less active than rosiglitazone but showed an efficacy comparable with (*S*)-**1**. In addition, (*S*)-**6** displayed potency about 7- and 5-fold higher than (*R*)-**6** (0.12 vs. 0.89 μM) and lead compound (*S*)-**1** (0.12 vs. 0.55 μM), respectively. Even though (*S*)-**1** and (*R*)-**1** were completely inactive on PPARδ,[35] we decided to test (*S*)-**6** on this subtype, but also in this case no activation was observed (data not shown). Therefore, given that (*S*)-**1** and (*R*)-**1** did not even affect the transcriptional activity of other nuclear receptors,[35] it is reasonable to assert that (*S*)-**6** is a PPARα/γ selective ligand.

On the basis of these results, we decided to investigate the interaction mode of (*S*)-**6** (hereafter LJ570) with both PPARα and PPARγ and, for this reason, we tried to resolve the X-ray structures of the corresponding complexes.

Binding of LJ570 to PPARα and PPARγ

Unfortunately, we could not resolve the crystal structure of LJ570 in the complex with PPARα, therefore, in order to gain insight into the possible binding mode, we undertook docking experiments whose results are reported in Supporting Information.

On the contrary, two structures of PPARγ-LBD with the ligand LJ570 were collected and solved from crystals obtained with different soaking times and ligand concentrations. In the first structure (short-term soaking time and low ligand concentration) the ligand occupies the region between the helix 3 (H3) and the β-sheet, in the canonical way as other known partial agonists and (*R*)-**1** (Fig. 4A).[21,23,24,26,35] The carboxylate group interacts with the NH of S342 via H-bonds mediated by one molecule of water. In the second structure (long-term soaking time and high ligand concentration), LJ570 interacts directly with Y473 of helix 12 (H12) and the two histidines of the canonical triad (H323 and H449) through H-bonds made by its carboxylate and occupies the diphenyl pocket, shifting the side-chain of F282, with one of its diphenyl groups in the same position assumed by the ligand (*S*)-**1** (Fig. 4B).[35] The two different positions of the ligand in the PPARγ-LBD obtained from different soaking times allow to suppose the existence of an equilibrium between two binding modes, both belonging to the canonical site, which resemble those of the two simultaneously bound molecules of an *iso*-propyl derivative of (*S*)-**1** (PDB code 4E4K).[30] Similar binding modes were also observed in the crystal structure of PPARγ with the partial agonist 2-chloro-N-(3-chloro-4-(5-chlorobenzo[*d*]thiazol-2-ylthio)phenyl)-4-(trifluoromethyl)benzenesulfonamide (T2384, PDB code 3K8S), also bound with two molecules in the canonical site of the LBD.[38,39] This latter compound, which displays unique biochemical and cellular activities together with an attractive *in vivo* profile, is considered a prototype for a novel class of PPARγ ligands with better therapeutic properties for treatment of type 2 diabetes. This prompted us to further investigate the biological activity of LJ570. To this end, we first determined whether this ligand could induce the differentiation of 3T3-L1 adipocytes, as a read out predictive of one of the major side effects of PPARγ full agonists like rosiglitazone (i.e., adipogenesis-mediated weight gain).

Effects of LJ570 on gene expression

To determine whether the particular interaction between LJ570 and PPARγ ligand-binding domain

could affect its adipogenic potential in vitro, 3T3-L1 fibroblasts were induced to differentiate to adipocytes with medium containing both LJ570 and insulin. Rosiglitazone was used as reference compound. Interestingly, LJ570 did not activate the PPARγ dependent program of adipocyte differentiation in 3T3-L1 cells. We did not observe any significant increased expression of fatty acid binding protein 4 (Fabp4), adiponectin (Adipoq), insulin-sensitive glucose transporter 4 (Glut4), class B scavenger receptor (Cd36), phosphoenolpyruvate carboxykinase 1 (Pck1), glycerol kinase (Gk), isocitrate dehydrogenase subunit alpha (Idh3a), and succinyl-CoA ligase subunit alpha (Suclg1) (Fig. 1A of Supporting Information). In accordance with these results, treatment of 3T3-L1 cells with LJ570 induced only very little lipid accumulation even at the highest tested concentration as compared to rosiglitazone, further indicating that LJ570 features much lower adipogenic activity than a full PPARγ agonist (Fig. 5, A and B). The activity of LJ570 on PPARα was determined in vitro by treating Hepa1-6 cells with three different concentrations of the ligand, using Wy-14,643 as reference compound. In this case, as expected, LJ570 increased the expression of three different PPARα-target genes: acyl-Coenzyme A oxidase 1 (Acox1), carnitine palmitoyltransferase 1a (Cpt1a) and acyl-Coenzyme A dehydrogenase, medium chain (Acadm) (Fig. 1B of Supporting Information). The effects on the expression of these three genes, which are essential for the peroxisomal and mitochondrial β-oxidation of fatty acids, allow to hypothesize a beneficial pharmacological profile of this compound on lipid metabolism.

Co-regulator recruitment by Fluorescence Resonance Energy Transfer assay

To further confirm the ability of LJ570 to interact with PPARγ, in spite of the lacking activation of some PPARγ target genes, we investigated the effects of its interaction on the coactivator recruitment from the ligand-activated receptor. To this end, we measured coactivator recruitment by FRET assay both in the absence and in the presence of rosiglitazone. The assay confirmed that LJ570 is able to recruit the PGC1α coactivator peptide on PPARγ (Fig. 6), although only at concentration higher than 1 μM, thus providing an additional evidence of its ability to interact with

the receptor. Interestingly, in the presence of three different concentrations of rosiglitazone (0.37, 1, and 10 microM), LJ570 induced a synergistic recruitment of PGC1α on the receptor (Fig. 6). This result prompted us to investigate the possibility that this ligand could bind, in the presence of rosiglitazone, to an alternate binding site. In fact, recently, Hughes et al. demonstrated that some synthetic PPARγ ligands not only bind to the canonical pocket at high affinity but can also bind to an alternate binding site at lower affinity, which is a surface exposed region capped by the conformationally flexible Ω-loop located between helix 2′ and helix 3, and affect PPARγ function.[40] Ligand binding to this latter site does not compete with endogenous ligand binding to the canonical site, indicating it is an alternate site. To determine if the origin of the synergistic recruitment of PGC1α on PPARγ was due to the simultaneous binding of rosiglitazone and LJ570 to the canonical and alternate sites, respectively, we performed a cotransfection assay by preincubating cells with **7** (GW9662, Fig. 7, upper part) before treating cells with ligand. **7** is a commercially available PPARγ antagonist that binds to the canonical site of PPARγ through a covalent thioether bond with C285 (Fig. 4C).[41] It was previously showed that **7** blocks the binding of many PPARγ ligands, including rosiglitazone, to the canonical site, whereas no effect has been reported on the alternate site.[40] In our experiment, as shown in Fig. 7A, the presence of **7** induced only a slight decrease in the potency of LJ570 allowing to suppose its binding to the alternate site with affinity similar to that for the canonical site. On the contrary, **7** blocked the action of rosiglitazone at concentrations up to 100 nM and only higher concentrations elicited an increase in PPARγ transactivation (Fig. 7B). In this case, the activation from rosiglitazone occurs through the alternate site too even though by a lower affinity binding as previously reported.[40] It is important to highlight that the two different positions which LJ570 can assume, as reported above, in the PPARγ-LBD are almost symmetrical, with a diphenyl group occupying, in both cases, the central region of LBD in front of C285 of H3 (Fig. 4C). Both positions show a common binding region with the antagonist **7** (Fig. 4C), covalently bound to C285 in the canonical site. Therefore, it is logical to hypothesize that the residual activity of LJ570, observed in the presence of **7**, might be possible only if the ligand occupies the alternate

binding site. On the other hand, this interaction would also explain the effects showed in Fig. 6: the higher the concentration of rosiglitazone, the lower the synergistic recruitment of PGC1α on the receptor; that is, at higher concentration, rosiglitazone would also occupy the alternate site limiting or preventing the accommodation of LJ570.

As a whole, it seems reasonable to assert LJ570 is able to interact with PPARγ through binding two molar equivalents: one to the canonical binding pocket at high affinity, where the ligand is in equilibrium between two different positions (Fig. 4C), and a second to the alternate site at a lower but potentially pharmacologically relevant affinity. However, even though the interaction with the alternate site occurs only at higher concentrations, its functional effects should not be overlooked. In fact, for *in vivo* animal model studies, PPARγ ligands are often administered several times a day over many months. In these cases, it is possible that ligand concentrations could be high enough to elicit an alternate site functional effect through binding a second molecule of the ligand. Although the pharmacological utility of the PPARγ alternate site remains unclear, it is possible that ligands binding this site might favor a correct balance of coactivator and corepressor binding or synergize with endogenous canonical ligands to provide a unique functional activity profile. As a matter of fact, it is logical to presume that the slight decrease on PPARγ activation shown by LJ570 after pretreatment with **7** in the luciferase reporter assay is the result of the occupation of the alternate site. In order to support this hypothesis, we decided to perform docking experiments to investigate on putative binding mode of LJ570 in the **7**-bound PPARγ-LBD.

Docking experiments

To further examine the possibility that LJ570 can bind to the alternate site in **7**-bound PPARγ-LBD, a molecular docking simulation was performed using the GOLD Suite docking package.[42] The crystal structure of human **7**-bound PPARγ-LBD was retrieved from the RCSB Protein Data Bank (PDB code 3B0R). However, this structure lacks the Ω-loop, a flexible region between H2′ and H3 (residues 262-274), which comprises part of the alternate site and synergistically affects PPARγ

structure and function.[43] Moreover, recent studies[43e,44] suggest that the Ω-loop may adopt different "closed" conformations according to the ligands that occupy the alternate binding site to achieve an optimal fit of the PPARγ-LBD with the ligand and to inhibit S273 phosphorylation by blocking Cdk5 from binding to the PPARγ LBD. For these reasons, we systematically scrutinized the PDB structures of PPARγ complexed with ligands occupying the alternate site in order to assess which conformation of the Ω-loop should be used to assemble the final receptor model. Finally, the PPARγ/S35 complex (PDB code 5GTO) was chosen as the best structure available in which the electron density for the flexible Ω-loop was clearly observed.[43e] So, the starting **7**-bound PPARγ crystal structure was modified to include the 12 missing residues (residues 262-274) in a surface loop structure (see Experimental procedures).

From results of our docking simulation, LJ570 in the presence of **7** is predicted to occupy the alternate ligand-binding site (Fig. 8A), which was previously identified by Hughes et al.[39] and visualized by X-ray crystallography.[43e,f] No steric clash is observed between LJ570 in the alternate site and **7** and, thus, both ligands can be accommodated simultaneously into the PPARγ-LBD. In Fig. 8B the overlap between the two positions of LJ570, in the canonical site, and the docked LJ570 occupying the alternate site is shown.

The interactions between LJ570 and the PPARγ-LBD involve one H-bond and several hydrophobic interactions. Specifically, one of the carboxylate oxygens of LJ570 forms a H-bond with the backbone nitrogen of S342 on the β-sheet with a distance of 3.3 Å. The hydrophobic interactions of LJ570 with the PPARγ-LBD can be divided in two groups. The first group occurs between the oxy-diphenyl group of LJ570 and V339, I341, M348 on the β-sheet, L330 on helix 5, and M364 on helix 7 in the binding pocket of known partial agonists. The second group of hydrophobic interactions involves the remaining diphenyl moiety of LJ570 and residues F264, I267, P269 (part of the Ω-loop), R280, G284, and F287 (helix 3) in the alternate site. Interestingly, the terminal phenyl ring of LJ570 forms stacking interactions with F287 from helix H3 and P269 of the Ω loop.

Notably, when we superimposed our LJ570-bound PPARγ-LBD complex onto the structures of S35 (PDB: 5GTO) and SR1664 (PDB: 5DWL) that bind to the PPARγ alternate site (Fig. 8C), we observed that the three compounds occupy a similar position in the LBD, contacting the helix H3 and the Ω-loop residues. While this work was in preparation, Kojetin and coworkers released a crystal structure of PPARγ bound to edaglitazone at the canonical pocket and nonanoic acid co-bound to the alternate site (PDB code: 5UGM).[45] Interestingly, the diphenyl moiety of LJ570 overlaps with the crystallized binding mode of nonanoic acid, whereas the carboxylate groups of both ligands are engaged in H-bonding to the S342 backbone (Fig. 8D).

Effects of LJ570 on Cdk5-mediated phosphorylation at S273 of PPARγ

The different PPARγ binding modes of the full and partial agonists do not fully explain their ability to exert antidiabetic properties. In 2010, Choi et al. described[21] a new antidiabetic mechanism of PPARγ-targeted drugs which depends upon the inhibition of PPARγ S273 phosphorylation by cyclin dependent kinase 5 (Cdk5). S273 phosphorylation results in the dysregulation of a subset of PPARγ target genes that are known to be associated with tissue insulin sensitization, whereas its inhibition maintains unchanged the transcription of several of these genes and the correlated insulin sensitization. However, the Cdk5-mediated phosphorylation of PPARγ does not have any influence on its transactivation activity and its role in adipocyte differentiation, which means that any ligand acting as inhibitor of this phosphorylation mechanism, would be able to exert antidiabetic effects. Therefore, this new mechanistic scenario might explain why some PPARγ partial agonists or modulators can exhibit antidiabetic effects similar to TZDs and other full agonists, without showing their typical side effects; that is, it has been proposed that the antidiabetic activity of PPARγ ligands occurs through the inhibitory effect on Cdk5-mediated phosphorylation of PPARγ, whereas the different potency and efficacy as agonists could be related to the different side-effect profiles. For this reason, we assessed the ability of LJ570 to inhibit Cdk5-mediated phosphorylation of PPARγ in vitro. For detecting and quantifying the possible inhibition rate, an ELISA (enzyme-linked

immunosorbent assay) protocol was optimized. As shown in Fig. 9, LJ570 effectively inhibited S273 phosphorylation with higher concentrations being more efficacious than rosiglitazone. This could be explained by taking into account the capability of LJ570 to assume two different positions: the former in the region between H3 and the β-sheet, in the canonical way as other known partial agonists and selective PPARγ modulators,[21,23,24,26] the latter in the alternate site by accommodating in a hydrophobic region between helices 2' and 3, the Ω -loop and the β3–β4 strands. In both cases, LJ570 would stabilize the β-sheet region of the PPARγ-LBD thus shielding S273 from Cdk5-mediated phosphorylation due to the location of S273 adjacent to the first β-strand of PPARγ, which is part of the Cdk5 recognition site.[21]

Effect of LJ570 on adipocyte glucose uptake

We finally tested the insulin-sensitizing effect of LJ570 by investigating its ability to increase glucose uptake in 3T3-L1 adipocytes. In fact, for some selective PPARγ modulators it has been demonstrated the possibility to dissociate the effects of PPARγ activation on adipogenesis from glucose uptake stimulation.[46] Therefore, we treated differentiated 3T3-L1 adipocytes with LJ570 and measured glucose uptake. As shown in Fig. 10A, LJ570 significantly increased the insulin-stimulated glucose uptake suggesting that its binding to PPARγ results in a biological effect that may improve insulin sensitivity. In spite of its potency as a PPARγ agonist, LJ570 stimulated glucose uptake only at concentration as high as 10 μM. At this concentration it is reasonable to suppose the interaction of PPARγ with two molecules of the ligand, the former in the canonical site and the latter in the alternate one, which cooperatively produce the resulting effect. However, to further confirm that this effect is also due to the interaction of LJ570 with the alternate site, we repeated the glucose uptake assay in the presence of 0.3 μM rosiglitazone and 10 μM LJ570. The concentration of both ligands was chosen on the basis of the additive effect shown, at these doses, on the recruitment of the PGC1α coactivator peptide (Fig. 6). As expected, the results of this new

experiment demonstrated that the combined treatment significantly increased the insulin-stimulated glucose uptake compared to the treatment with either drug administered alone (Fig. 10B).

At this point, we decided to verify the presence of a potential weak effect of LJ570 on the expression of the PPARγ target genes involved in the PPARγ-dependent program of adipocyte differentiation also at 5 and 10 μM given that previous experiments were conducted at concentration up to 2.5 μM. Again, even at this concentration, LJ570 did not induce any significant increased expression of Fabp4, Adipoq, Glut4, and Pck1 (Fig. 1C of Supporting Information). In accordance with these results, treatment of 3T3-L1 cells with 10 μM LJ570 still induced much lower lipid accumulation as compared to rosiglitazone (Fig. 1D of Supporting Information).

Conclusion

In the present study, we investigated the effects resulting from the chemical modification of the previously reported PPAR ligand (*S*)-**1**. This allowed the identification of the new compound LJ570 able to potently activate both PPARα and γ subtypes as a partial agonist. However, in vitro experiments in 3T3-L1 pre-adipocyte cell line showed that LJ570 did not activate any of the PPARγ target genes involved in the PPARγ-dependent program of adipocyte differentiation. In accordance with these results, treatment of 3T3-L1 cells with LJ570 induced only very little lipid accumulation which is one of the major side effects of full agonists like rosiglitazone. However, an acute treatment of 3T3-L1 adipocytes with LJ570 increased the insulin-stimulated glucose uptake. In addition, LJ570 effectively inhibited Cdk5-mediated phosphorylation of PPARγ in vitro which has been recently described as a new mechanism through which some PPARγ-targeted partial agonists or antagonists are able to maintain their antidiabetic activity without showing the typical side effects of full agonists. On the contrary, LJ570 increased the expression of three typical PPARα target genes which are essential for the hepatic peroxisomal and mitochondrial β-oxidation of fatty acids, allowing to hypothesize a beneficial pharmacological profile of this compound on lipid

metabolism.

As far as we know, this ligand is the first PPARα/γ dual agonist reported to inhibit S273-phosphorylation of PPARγ and, therefore, may represent the potential lead of a new class of drugs with better pharmacological properties in the treatment of dyslipidemic type 2 diabetes.

Interestingly, X-ray studies of the complex PPARγ/LJ570 allowed to collect and solve two different structures from crystals obtained with different soaking times and ligand concentrations: the former, typical of the partial agonists and characterized by accommodation into the region between helix 3 and the β-sheet; the latter, in which the ligand is situated more deeply in the PPARγ-LBD assuming a position more similar to full agonists. It is reasonable to suppose that the activity of the ligand is the result of an equilibrium between these two different binding modes, both belonging to the canonical pocket. However, LJ570 seems also to be able to bind an alternate site as demonstrated from its activity on PPARγ even in the presence of a specific irreversible antagonist and the capability to induce a synergistic recruitment of PGC1α on PPARγ and an additive effect on glucose uptake in the presence of rosiglitazone. Even though the interaction of LJ570 with this alternate site occurs only at high, but pharmacologically relevant, concentration, it could account for its activity profile. In fact, although the pharmacological utility of the PPARγ alternate site remains unclear, it is possible that ligands bound to this site contribute to regulate receptor activity allowing to fine tune the functional response of PPARγ without competing, but rather synergizing, with endogenous canonical ligands. Thus, the development of a new generation of PPARγ drugs as alternate modulators targeting non-canonical sites of the ligand binding domain could be a promising approach to address selectivity concerns and therapeutic profile.

EXPERIMENTAL SECTION

Chemical Methods. Column chromatography was performed on ICN Silica Gel 60 Å (63−200 μm) as a stationary phase. Melting points were determined in open capillaries on a Gallenkamp electrothermal apparatus and are uncorrected. Mass spectra were recorded on an HP GC/MS 6890-5973 MSD spectrometer, electron impact 70 eV, equipped with an HP chemstation or an Agilent LC/MS 1100 series LC/MSD Trap System VL spectrometer, electrospray ionization (ESI). ^{1}H-NMR spectra were recorded in CDCl$_3$ (the use of other solvents is specified) on a Varian-Mercury 300 (300 MHz) spectrometer at room temperature. Chemical shifts are expressed as parts per million (δ). The purity of all tested compounds was > 95%, as confirmed by combustion analysis carried out with a Eurovector Euro EA 3000 model analyzer. For optical isomers, MS and NMR spectra are reported only for the racemate or one of the stereoisomers. Optical rotations were measured with a Perkin-Elmer 341 polarimeter at room temperature (20 °C): concentrations are expressed as grams per 100 mL. The enantiomeric excesses of the final acids were determined by HPLC analysis on a Chiralcel OD or AD column (4.6 mm i.d. × 250 mm, Daicel Chemical Industries, Ltd., Tokyo, Japan). Analytical liquid chromatography was performed on a PE chromatograph equipped with a Rheodyne 7725i model injector, a 785A model UV/vis detector, a series 200 model pump, and an NCI 900 model interface. Chemicals were from Aldrich (Milan, Italy), AlfaAesar (Karlsruhe, Germany), or Acros (Milan, Italy) and were used without any further purification.

Ethyl 2-(1,1'-diphenyl-4'-ol-4-oxy)-3-phenyl-propanoate (2a).

A solution of diisopropylazodicarboxylate (DIAD, 5 mmol) in anhydrous THF (10 mL) was added dropwise to an ice-bath cooled mixture of (*R,S*)-ethyl phenyllactate (5 mmol), 4,4'-dihydroxydiphenyl (5 mmol), and triphenylphosphine (5 mmol) in anhydrous THF (20 mL). The reaction mixture was stirred at room temperature overnight, under N$_2$ atmosphere. THF was evaporated in vacuo, and the residue was chromatographed on silica gel column (petroleum ether/ethyl acetate 9:1 as eluent) affording the desired compound as a white solid in 41% yields.

GC-MS m/z (%): 362 (M$^+$, 100), 289 (9), 186 (65). ^{1}H-NMR (CDCl$_3$): δ 1.20 (t, 3H, J=7.15, CH$_3$), 3.21-3.30 (m, 2H, CH$_2$-Ph), 4.19 (q, 2H, J=7.15, CH$_2$-O), 4.80-4.84 (dd, 1H, CH), 5.03 (s, 1H, OH, D$_2$O exchanged), 6.82-6.88 (m, 4H, aromatics), 7.24-7.40 (m, 9H, aromatics).

Ethyl 2-[4-[4-(1-ethoxy-1-oxopropan-3-phenyl-2-yl)oxyphenyl]phenoxy]-3-phenyl-propanoate (2b).

The title compound was obtained as a white solid in 30% yield by using the same procedure reported above starting from **2a** and another equivalent amount of (*R,S*)-ethyl phenyllactate. GC-MS m/z (%): 538 (M$^+$, 100) 465 (8), 362 (6). ^{1}H-NMR (CDCl$_3$): δ 1.20 (t, 6H, J=7.15, 2 CH$_3$), 3.21-3.30 (m, 4H, 2 CH$_2$-Ph), 4.19 (q, 4H, J=7.15, 2 CH$_2$-O), 4.80-4.84 (m, 2H, 2 CH), 6.82-6.88 (m, 4H, aromatics), 7.24-7.40 (m, 14H, aromatics).

2-[4-[4-(1-Carboxy-2-phenylethoxy)phenyl]phenoxy]-3-phenyl-propanoic acid (2).

A solution of **2b** (1 mmol) in THF (10 mL) and 1 N NaOH (10 mL) was stirred at room temperature for 3 h. The organic layer was removed under reduced pressure, and the residue was acidified with 2 N HCl and extracted with Et$_2$O. The organic layer was dried over Na$_2$SO$_4$ and evaporated to dryness affording the final acid as a white solid which was crystallized from AcOEt/hexane (55% yields). Mp: 138-140 °C; GC-MS, (methyl ester) m/z (%): 510 (M$^+$, 49) 451 (4), 121 (100). ^{1}H-NMR (CDCl$_3$): δ 3.28 (d, 4H, J=6.32, 2 CH$_2$), 4.83 (t, 2H, J=6.32, 2 CH), 5.60-6.60 (bb, 2H, COOH, D$_2$O exchanged), 6.84-6.87 (m, 4H, aromatics), 7.22-7.36 (m, 14H, aromatics). Anal. Calcd for C$_{30}$H$_{26}$O$_6$: C, 74.67; H, 5.43. Found: C, 75.02; H, 5.81.

General Procedure for Synthesis of (*R,S*)-, (*R*)- or (*S*)-ethyl 2-(4-(4,4,5,5-tetramethyl-1,3,2-dioxaborolan-2-yl)phenoxy)-3-phenyl-propanoate ((*R,S*)-3a, (*R*)-3a, (*S*)-3a).

A solution of diisopropylazodicarboxylate (DIAD, 2 mmol) in anhydrous THF (7 mL) was added dropwise to an ice-bath cooled mixture of (*R,S*)-, (*S*)-or (*R*)-ethyl phenyllactate (2 mmol), 4-(4,4,5,5-tetramethyl-1,3,2-dioxaborolan-2-yl)phenol (2 mmol), and triphenylphosphine (3 mmol) in anhydrous THF (7 mL). The reaction mixture was stirred at room temperature for 48 h, under N$_2$

atmosphere. Then, the solvent was evaporated in vacuo and the residue was chromatographed on silica gel column (*n*-hexane/ethyl acetate 90:10 as eluent), affording a colorless oil. GC-MS m/z (%): 396 (M$^+$, 100), 223 (56), 177 (69), 135 (94). ^{1}H-NMR (CDCl$_3$): δ 1.16 (t, 3H, J=7.15, C*H$_3$*-CH$_2$-O), 1.31 (s, 12H, 4 CH$_3$C-O), 3.23-3.29 (m, 2H, Ar-C*H$_2$*-CH); 4.15 (q, 2H, J=7.15, CH$_3$-C*H$_2$*-O), 4.81-4.86 (m, 1H, CH); 6.81-6.85, 7.19-7.30 and 7.68-7.71 (m, 9H, aromatics).

 (***R,S***)-**3a.** Yield: 37%. (***R***)-**3a.** Yield: 17%. (***S***)-**3a.** Yield: 20%.

(R^IS^I, $R^{II}S^{II}$)- Ethyl 2-(diphenyl-4-yl-oxy)-3-[4'-(1-ethoxycarbonyl-2-phenyl-ethoxy)diphenyl-4-yl]propanoate ((R^IS^I, $R^{II}S^{II}$)-3b).

Compound (***R,S***)-**3a** (0.25 mmol), Cs$_2$CO$_3$ (0.25 mmol), and ethyl 2-(4-phenylphenoxy)-3-(4-bromophenyl)propanoate **6e** (0.16 mmol) were dissolved in anhydrous toluene (10 mL) at 95 °C, under N$_2$ atmosphere. After 0.5 h, Pd(PPh$_3$)$_4$ (0.0075 mmol) was added. The reaction mixture was stirred for 24 h at 95 °C and then quenched with 1 N HCl (2 mL) and ethyl acetate (2 mL). The suspension was filtered through a Celite pad to remove the catalyst, and the filtrate was washed with saturated NaHCO$_3$ solution and brine. The filtrate was concentrated under reduced pressure, dissolved in ethyl acetate, washed with brine, dried over Na$_2$SO$_4$, filtered, and evaporated to dryness to give an oily residue which was chromatographed on a silica gel column (*n*-hexane/ethyl acetate, 90:10, as eluent), affording the desired compound as a colorless oil. Yield: 39%. ESI-MS (positive) m/z (%): 637 (M+Na$^+$, 27), 569 (34), 391 (100). ^{1}H-NMR (CDCl$_3$): δ 1.16-1.23 (m, 6H, 2 CH$_3$), 3.24-3.30 (m, 4H, 2 CH$_2$-Ar), 4.15-4.24 (m, 4H, 2 CH$_2$-O), 4.81-4.86 (m, 2H, 2 CH), 6.87-6.93 and 7.29-7.52 (m, 22H, aromatics).

Synthesis of the Stereoisomers of (R^IS^I, $R^{II}S^{II}$)-3b.

The title compounds were prepared by the same procedure reported above starting from (***R***)-**3a** or (***S***)-**3a** and (*R*)- or (*S*)-ethyl 2-(4-phenylphenoxy)-3-(4-iodophenyl)propanoate **6g**. (***S^IR^{II}***)-**3b**: 39% yield; (***R^IS^{II}***)-**3b**: 10% yield; (***S^IS^{II}***)-**3b**: 46% yield; (***R^IR^{II}***)-**3b**: 5% yield.

General Procedure for Synthesis of (R^IS^I, $R^{II}S^{II}$)-2-(diphenyl-4-yl-oxy)-3-[4'-(1-carboxy-2-phenylethoxy)diphenyl-4-yl]propanoic acid ((R^IS^I, $R^{II}S^{II}$)-3) and its Stereoisomers.

To a stirred solution of the corresponding diethyl ester (0.1 mmol) in THF (5 mL), 1 N NaOH (5 mL) was added. The reaction mixture was stirred overnight at room temperature. Then, the solvent was evaporated in vacuo and the aqueous phase was acidified with 2 N HCl and extracted with Et$_2$O. The combined organic layers were washed with brine, dried over Na$_2$SO$_4$ and evaporated to dryness affording the title diacids as white solids, which were recrystallized from CHCl$_3$/n-hexane. ESI-MS (negative) m/z (%): 557 (M-H, 1), 409 (8), 387 (100), 239 (51). ^{1}H-NMR (CDCl$_3$): δ 3.28-3.34 (m, 4H, 2 CH$_2$-Ar), 4.84-4.97 (m, 2H, 2 CH), 6.87-6.97 and 7.27-7.52 (m, 22H, aromatics).

The enantiomeric (*ee*) and diastereomeric excesses (*de*) of the stereoisomers were determined by using a CSP-HPLC column CHIRALCEL$^®$ AD; lambda = 254 nm; 1 mL/min; n-hexane/*iso*-propanol/TFA 80:20:0.2. (*R^IS^I, $R^{II}S^{II}$*)-3: 89% yield, mp 163-165 °C. Anal. Calcd for C$_{36}$H$_{30}$O$_6$: C, 77.40; H, 5.41. Found: C, 77.08; H, 5.42. (*S^IR^{II}*)-3: 88% yield, mp 198-200 °C, *ee* > 99%, *de* 87%; [α]$_D$ = + 31.5 (c 1.0, MeOH). Anal. Calcd for C$_{36}$H$_{30}$O$_6$: C, 77.40; H, 5.41. Found: C, 77.17; H, 5.40. (*R^IS^{II}*)-3: 26% yield, mp 169-170 °C, *ee* > 99%, *de* 90%; [α]$_D$ = - 32.4 (c 0.7, MeOH). Anal. Calcd for C$_{36}$H$_{30}$O$_6$: C, 77.40; H, 5.41. Found: C, 77.88; H, 5.62. (*S^IS^{II}*)-3: 46% yield, mp 205-207 °C, *ee* > 99%, *de* 92%; [α]$_D$ = + 37.5 (c 1.0, MeOH). Anal. Calcd for C$_{36}$H$_{30}$O$_6$: C, 77.40; H, 5.41. Found: C, 77.33; H, 5.52. (*R^IR^{II}*)-3: 88% yield, mp 164-167 °C, *ee* > 99%, *de* 90%; [α]$_D$ = - 38.7 (c 0.8, MeOH). Anal. Calcd for C$_{36}$H$_{30}$O$_6$: C, 77.40; H, 5.41. Found: C, 77.11; H, 5.75.

General Procedure for Synthesis of ethyl 2-(4-(4,4,5,5-tetramethyl-1,3,2-dioxaborolan-2-yl)phenoxy)propanoate (4a) and ethyl (4-(4,4,5,5-tetramethyl-1,3,2-dioxaborolan-2-yl)phenoxy)acetate (5a).

4-(4,4,5,5-Tetramethyl-1,3,2-dioxaborolan-2-yl)phenol (0.9 mmol) was added to a suspension of cesium carbonate (1.8 mmol) in anhydrous THF (10 mL). After 0.5 h a solution of ethyl bromopropanoate or ethyl bromoacetate in anhydrous THF (5 mL) was added dropwise and the reaction mixture was refluxed for 6 h, under N$_2$ atmosphere. Then, the solvent was evaporated in vacuo and the residue dissolved in diethyl ether and washed twice with 1 N HCl and brine, dried

over Na_2SO_4 and evaporated to dryness. The oily residue was chromatographed on a silica gel column (*n*-hexane/ethyl acetate 90:10 as eluent) affording a colorless oil.

Ethyl 2-(4-(4,4,5,5-tetramethyl-1,3,2-dioxaborolan-2-yl)phenoxy)propanoate (4a).

Yield: 37%. GC-MS m/z (%): 320 (M$^+$, 41), 247 (100). ^{1}H-NMR (CDCl$_3$): δ 1.23 (t, 3H, J=7.15, C*H$_3$*-CH$_2$-O); 1.32 (s, 12H, 4 CH$_3$C); 1.61 (d, 3H, J=6.97, C*H$_3$*CH); 4.20 (q, 2H, J=7.15, CH$_2$); 4.81 (q, 1H, J=6.97, CH), 6.84-6.88 and 7.71-7.74 (m, 4H, aromatics).

Ethyl (4-(4,4,5,5-tetramethyl-1,3,2-dioxaborolan-2-yl)phenoxy)acetate (5a).

Yield: 56%. GC-MS m/z (%): 306 (M$^+$, 100). ^{1}H-NMR (CDCl$_3$): δ 1.28 (t, 3H, J=7.15, C*H$_3$*-CH$_2$-O); 1.33 (s, 12H, 4 CH$_3$C); 4.26 (q, 2H, J=7.15, CH$_3$-C*H$_2$*-O); 4.64 (s, 2H, O-CH$_2$-CO), 6.88-6.91 and 7.74-7.77 (m, 4H, aromatics).

General Procedure for Synthesis of ethyl 2-(diphenyl-4-yl-oxy)-3-[4'-(1-ethoxycarbonyl-ethoxy)diphenyl-4-yl]propanoate (4b) and 2-(diphenyl-4-yl-oxy)-3-[4'-(ethoxycarbonyl-methoxy)diphenyl-4-yl]propanoate (5b).

Compound **4a** or **5a** (0.34 mmol), Cs$_2$CO$_3$ (0.51 mmol), and **6e** (0.34 mmol) were dissolved in anhydrous toluene (8 mL) at 95 °C, under N$_2$ atmosphere. After 0.5 h, Pd(PPh$_3$)$_4$ (0.01 mmol) was added. The reaction mixture was stirred for 20 h at 95 °C and then quenched with 1 N HCl (3 mL) and ethyl acetate (3 mL). The suspension was filtered through a Celite pad to remove the catalyst, and the filtrate was washed with saturated NaHCO$_3$ solution and brine. The filtrate was concentrated under reduced pressure, dissolved in ethyl acetate, washed with brine, dried over Na$_2$SO$_4$, filtered, and evaporated to dryness to give an oily residue which was chromatographed on a silica gel column (*n*-hexane/ethyl acetate, 90:10, as eluent), affording the desired compounds as colorless oils.

Ethyl 2-(diphenyl-4-yl-oxy)-3-[4'-(1-ethoxycarbonyl-ethoxy)diphenyl-4-yl]propanoate (4b).

Yield: 41%. ESI-MS (positive) m/z (%): 561 (M+Na$^+$, 100); ^{1}H-NMR (CDCl$_3$): δ 1.19-1.28 (m, 6H, 2 C*H$_3$*-CH$_2$), 1.64 (d, 3H, J=6.88, CH-C*H$_3$*), 3.23-3.36 (m, 2H, CH$_2$-Ar), 4.18-4.27 (m, 4H, 2

CH$_2$-O), 4.77 (q, 1H, J=6.88, CH-CH$_3$), 4.83-4.87 (dd, 1H, CH-CH$_2$), 6.91-6.94 and 7.29-7.53 (m, 17H, aromatics).

Ethyl 2-(diphenyl-4-yl-oxy)-3-[4'-(ethoxycarbonyl-methoxy)diphenyl-4-yl]propanoate (5b).

Yield: 56%. ESI-MS (positive) m/z (%): 547 (M+Na$^+$, 100); ^{1}H-NMR (CDCl$_3$): δ 1.22 and 1.31 (2t, 6H, J=7.15, 2 CH_3-CH$_2$), 3.23-3.36 (m, 2H, CH$_2$-Ar), 4.66 (s, 2H, CH$_2$-O), 4.15 and 4.23 (2q, 4H, J=7.15, 2 CH$_3$-CH_2), 4.83-4.88 (dd, 1H, CH), 6.91-6.98 and 7.29-7.52 (m, 17H, aromatics).

General Procedure for Synthesis of 2-(diphenyl-4-yl-oxy)-3-[4'-(1-carboxy-ethoxy)diphenyl-4-yl]propanoic acid (4) and 2-(diphenyl-4-yl-oxy)-3-[4'-(carboxy-methoxy)diphenyl-4-yl]propanoic acid (5).

To a stirred solution of the corresponding diethyl ester (0.15 mmol) in THF (10 mL), 1 N NaOH (10 mL) was added. The reaction mixture was stirred for 3 h at room temperature. Then, the solvent was evaporated in vacuo and the aqueous phase was acidified with 6 N HCl (2 ml) and extracted with diethyl ether. The combined organic layers were washed with brine, dried over Na$_2$SO$_4$ and evaporated to dryness affording the title acids as white solids, which was crystallized from CHCl$_3$/n-hexane.

2-(Diphenyl-4-yl-oxy)-3-[4'-(1-carboxy-ethoxy)diphenyl-4-yl]propanoic acid (4).

Yield = 30%. Mp = 163-169 °C. ESI-MS (negative) m/z (%): 481 (M-H, 100); ^{1}H-NMR (DMSO-d_6): δ 1.49 (d, 3H, J=6.60, CH-CH_3), 3.12-3.48 (m, 2H, CH$_2$-Ar), 4.84 (q, 1H, J=6.60, CH-CH$_3$), 4.99-5.03 (dd, 1H, CH-CH$_2$), 6.89-6.94 and 7.25-7.57 (m, 17H, aromatics). Anal. Calcd for C$_{30}$H$_{26}$O$_6$: C, 76.67; H, 5.43. Found: C, 76.98; H, 5.37.

2-(Diphenyl-4-yl-oxy)-3-[4'-(carboxy-methoxy)diphenyl-4-yl]propanoic acid (5).

Yield = 36%. Mp = 188-194 °C. ESI-MS (negative) m/z (%): 467 (M-H, 100); ^{1}H-NMR (DMSO-d_6): δ 3.13-3.31 (m, 2H, CH-CH_2), 4.68 (s, 2H, CH$_2$-O), 4.98-5.03 (m, 1H, CH), 6.92-6.97 and 7.25-7.57 (m, 17H, aromatics). Anal. Calcd for C$_{29}$H$_{24}$O$_6$: C, 74.35; H, 5.16. Found: C, 73.74; H, 5.13.

Diethyl 2-(4-phenyl-phenoxy)malonate (6a).

A mixture of diethyl chloromalonate (14.4 mmol) and sodium 4-phenylphenate (15.8 mmol), prepared from an equivalent amount of 4-phenylphenol and sodium in absolute EtOH, was stirred and heated under reflux in acetone (115 mL) for 6 h. The solvent was evaporated under reduced pressure, and the residue was taken up with ethyl acetate, washed twice with 0.5 N NaOH and brine, dried over Na_2SO_4 and concentrated to give an oily residue which was chromatographed on silica gel column (*n*-hexane/ethyl acetate 95:5 as eluent). The title compound was obtained as a white solid in 78% yield. GC-MS m/z (%): 328 (M^+, 100), 169 (47), 152 (38). ^{1}H-NMR (CDCl$_3$): δ 1.32 (t, 6H, J=7.15, 2 CH$_3$), 4.33 (q, 4H, J=7.15, 2 CH$_2$), 5.24 (s, 1H, CH), 7.02-7.06 and 7.25-7.55 (m, 9H, aromatics).

Diethyl 2-(4-phenyl-phenoxy)-2-(4-bromo-benzyl)malonate (6b).

A solution of **6a** (11.4 mmol) in anhydrous DMF (15 mL) was added dropwise to a suspension of NaH (95% powder, 34.0 mmol) in the same solvent (30 mL) at 0 °C. After stirring for 20 min at rt, a solution of 4-bromo-benzylbromide (22.8 mmol) in anhydrous DMF (15 mL) was added dropwise and the resulting reaction mixture stirred at 55 °C for 24 h. DMF was removed under reduced pressure and the residue was dissolved in ethyl acetate, washed twice with saturated ammonium chloride solution and brine. The organic phase was dried over Na_2SO_4 and the solvent evaporated in vacuo to give a white solid which was chromatographed on silica gel column (*n*-hexane/ethyl acetate 98:2 as eluent). The title compound was obtained as a colorless oil in 63% yield. GC-MS m/z (%): 498 (M^++2, 1), 496 (M^+, 1), 170 (100). ^{1}H-NMR (CDCl$_3$): δ 1.15 (t, 6H, J=7.15, 2 CH$_3$), 3.61 (s, 2H, CH$_2$-Ph), 4.19 (q, 4H, J=7.15, 2 CH$_2$-O), 7.02-7.12 and 7.25-7.56 (m, 13H, aromatics).

Diethyl 2-(4-phenyl-phenoxy)-2-(4-phenyl-benzyl)malonate (6c).

Phenylboronic acid (2.0 mmol) and Cs$_2$CO$_3$ (1.5 mmol) were added, under N$_2$ atmosphere, to a stirred solution of **6b** (1 mmol) in anhydrous toluene (18 mL). After 0.5 h, Pd(PPh$_3$)$_4$ (0.03 mmol) was added, and the reaction mixture was stirred for 24 h at 95 °C. Then, it was quenched with 1 N

HCl (5 mL) and ethyl acetate (5 mL) and filtered through a Celite pad to remove the catalyst. The filtrate was washed twice with saturated NaHCO$_3$ solution and brine, dried over Na$_2$SO$_4$, and concentrated to dryness to give a yellow solid residue which was chromatographed on a silica gel column, (*n*-hexane/diethyl ether 90:10 as eluent), affording the title compound as a white solid. Yield: 40%. ESI-MS (positive) m/z (%): 517 (M+Na, 100), 348 (2). ^{1}H-NMR (CDCl$_3$): δ 1.16 (t, 6H, J=7.15, 2 CH$_3$), 3.70 (s, 2H, CH$_2$-Ph), 4.21 (q, 4H, J=7.15, 2 CH$_2$-O), 7.05-7.10 and 7.29-7.58 (m, 18H, aromatics).

(*R*,*S*)-2-(4-Phenyl-phenoxy)-3-(4-diphenyl)propanoic acid (6).

The diester **6c** (7.0 mmol) was stirred and refluxed with 1 N NaOH (21 mL) in 95% EtOH (70 mL) for 18 h. The organic solvent was distilled off under reduced pressure and the resulting aqueous phase was acidified to pH 2 with 6 N HCl and extracted with Et$_2$O (5x50 ml). The combined organic extracts were washed with brine, dried over Na$_2$SO$_4$ and the solvent removed under reduced pressure. The resulting mixture was heated at 160 °C for 2 h affording the desired acid as a white solid which was crystallized from CHCl$_3$/n-hexane (61% yield). Mp > 200°C. ESI-MS (negative) m/z (%): 393 (M-H, 100), 223 (32), 169 (24). ^{1}H-NMR (DMSO-d_6): δ 3.15-3.48 (m, 2H, CH$_2$), 5.00-5.04 (dd, 1H, CH), 6.92-6.95 and 7.25-7.64 (m, 18H, aromatics). Anal. Calcd for C$_{27}$H$_{22}$O$_3$: C, 82.21; H, 5.62. Found: C, 81.97; H, 5.50.

(*R*,*S*)-2-(4-Phenyl-phenoxy)-3-(4-bromophenyl)propanoic acid (6d).

The title compound was obtained as a white solid in 35% yield by using the procedure described above for **6**. ESI-MS (negative) m/z (%): 395 (M-H, 100), 225 (43), 169 (59). ^{1}H-NMR (CDCl$_3$): δ 3.20-3.28 (m, 2H, CH$_2$), 4.84-4.97 (dd, 1H, CH), 6.90-6.94 and 7.15-7.55 (m, 13H, aromatics).

Ethyl 2-(4-phenyl-phenoxy)-3-(4-bromophenyl)propanoate (6e).

The acid **6d** (1 mmol) was dissolved in 96° ethanol (20 mL) at 80 °C and added with 3 drops of concentrated sulfuric acid. The reaction mixture was refluxed for 5 h. Then, the solvent was evaporated, and the residue was dissolved in ethyl acetate, washed with saturated NaHCO$_3$ solution

and brine. The organic phase was dried over Na_2SO_4, filtered and concentrated under reduced pressure affording a white solid (0.67 mmol). Yield: 67%. GC-MS m/z (%): 426 (M^++2, 60), 424 (M^+, 58), 170 (100). ^{1}H-NMR ($CDCl_3$): δ 1.22 (t, 3H, J=7.15, CH_3), 3.18-3.28 (m, 2H, CH_2Ph), 4.20 (q, 2H, J=7.15, CH_2-O), 4.68-4.81 (dd, 1H, CH), 6.87-6.92 and 7.19-7.53 (m, 13H, aromatics).

General Procedure for Synthesis of (*R*)- or (*S*)-ethyl 4-iodo-phenyllactate ((*R*)-6f, (*S*)-6f).

1 N HCl (6 mL) and glacial acetic acid (9 mL) were added to a suspension of commercially available (*R*)- or (*S*)-(4-iodo)phenylalanine (5 mmol) in H_2O (17 mL). The resulting solution was stirred and cooled to 0 °C and carefully added, during 0.5 h, of $NaNO_2$ (42 mmol) solution in H_2O (9 mL). The solution was stirred at room temperature for 22 h and carefully added, during 0.5 h, of concentrated HCl (5 mL). Water was distilled off and the residue was extracted six times with boiling acetone. Acetone was distilled off and the oily residue was dissolved in Et_2O and dried over Na_2SO_4. The solvent was evaporated to dryness affording the corresponding (*R*)- or (*S*)-(4-iodo)phenyllactic acids as white solids. This solid was dissolved in absolute EtOH (30 mL), added of two drops of concentrated H_2SO_4 and refluxed with stirring for 5 h. The solvent was removed under reduced pressure, the residue was dissolved in Et_2O and the resulting solution was washed twice with saturated $NaHCO_3$ solution and brine. After drying over Na_2SO_4, the evaporation of the solvent afforded the corresponding ethyl esters as yellow oils which were used in the next step without any further purification. GC-MS m/z(%): 320 (M^+, 15), 302 (85), 217 (100), 91 (37).

General Procedure for Synthesis of (*R*)- or (*S*)-ethyl 2-(4-phenylphenoxy)-3-(4-iodophenyl)propanoate ((*R*)-6g, (*S*)-6g).

A solution of diisopropylazodicarboxylate (DIAD, 5 mmol) in anhydrous THF (8 mL) was added dropwise to an ice-bath cooled mixture of **(*S*)-6f** or **(*R*)-6f** (5 mmol), 4-phenyl-phenol (5 mmol), and triphenylphosphine (5 mmol) in anhydrous THF (8 mL). The reaction mixture was stirred at room temperature overnight, under N_2 atmosphere. Then, the solvent was evaporated in vacuo and the residue was chromatographed on silica gel column, (*n*-hexane/ethyl acetate 90:10 as eluent), affording a yellow solid (0.87 mmol). GC-MS m/z (%): 471 (M^+, 100), 170 (69). ^{1}H-NMR

(CDCl$_3$): 1.21 (t, 3H, J=6.90 CH$_3$); 3.19-3.21 (m, 2H, Ar-CH$_2$); 4.20 (q, 2H, J=6.90, CH$_3$-CH$_2$), 4.78-4.80 (m, 1H, CH), 6.87-7.64 (m. 13H, aromatics).

(**R**)-**6g.** Yield: 30%. (**S**)-**6g.** Yield: 37%.

General Procedure for Synthesis of (*R*)- or (*S*)-ethyl 2-(4-phenylphenoxy)-3-(4-diphenyl)propanoate ((*R*)-6h, (*S*)-6h).

Phenylboronic acid (0.84 mmol) and Cs$_2$CO$_3$ (0.63 mmol) were added, under N$_2$ atmosphere, to a stirred solution of (**R**)-**6g** or (**S**)-**6g** (0.42 mmol) in anhydrous toluene (10 mL). After 0.5 h, Pd(PPh$_3$)$_4$ (0.013 mmol) was added, and the reaction mixture was stirred for 35 h at 95 °C. Then, it was quenched with 1 N HCl (3 mL) and ethyl acetate (3 mL) and filtered through a Celite pad to remove the catalyst. The filtrate was washed twice with saturated NaHCO$_3$ solution and brine, dried over Na$_2$SO$_4$, and concentrated to dryness to give a dark yellow oily residue which was chromatographed on a silica gel column (*n*-hexane/ethyl acetate 90:10 as eluent) affording the title compounds as white solids. GC-MS m/z (%): 422 (M$^+$, 60), 253 (64), 167 (100). ^{1}H-NMR (CDCl$_3$): 1.22 (t, 3H, J=7.03, CH$_3$); 3.30-3.33 (m, 2H, Ar-CH$_2$); 4.22 (q, 2H, J=7.03, CH$_3$-CH$_2$), 4.86-4.90 (m, 1H, CH), 6.91-7.60 (m. 18H, aromatics).

(**R**)-**6h.** Yield: 40%. (**S**)-**6h.** Yield: 35%.

General Procedure for Synthesis of (*R*)- or (*S*)-2-(4-phenyl-phenoxy)-3-(4-diphenyl)propanoic acid ((*R*)-6, (*S*)-6).

To a stirred solution of (**R**)-**6h** or (**S**)-**6h** (0.15 mmol) in THF (7.5 mL), 1 N NaOH was added (7.5 mL). The reaction mixture was stirred overnight at room temperature. Then, the solvent was evaporated in vacuo and the aqueous phase was acidified with 2 N HCl and extracted with ethyl acetate. The combined organic layers were washed with brine, dried over Na$_2$SO$_4$ and evaporated to dryness affording the title acids as white solids, which were crystallized from CHCl$_3$/*n*-hexane. ESI-MS (negative) m/z (%): 393 (M–H, 100), 223 (32), 169 (24). ^{1}H-NMR (DMSO-*d$_6$*): δ 3.15-3.48 (m, 2H, CH$_2$), 5.00-5.04 (dd, 1H, CH), 6.92-6.95 and 7.25-7.64 (m, 18H, aromatics).

The enantiomeric excesses (*ee*) were determined by using a CSP-HPLC column CHIRALCEL®

OD; lambda = 254 nm; 1 mL/min; *n*-hexane/*iso*-propanol/TFA 95:5:0.1.

(*R*)-2-(4-Phenyl-phenoxy)-3-(4-diphenyl)propanoic acid ((*R*)-6).

Yield: 52%; mp = > 200 °C; *ee* = > 90%; $[\alpha]_D$ = - 37.5 (c 1.0, MeOH). Anal. Calcd for $C_{27}H_{22}O_3$:

C, 82.21; H, 5.62. Found: C, 82.20; H, 5.66.

(*S*)-2-(4-Phenyl-phenoxy)-3-(4-diphenyl)propanoic acid ((*S*)-6).

Yield: 65%; mp = 197-9 °C; *ee* = 90%; $[\alpha]_D$ = + 36.7 (c 1.0, MeOH). Anal. Calcd for $C_{27}H_{22}O_3$: C,

82.21; H, 5.62. Found: C, 82.60; H, 5.67.

Biological Methods. Reference compounds, the medium, and other cell culture reagents were

purchased from Sigma-Aldrich (Milan, Italy).

Plasmids. The expression vectors expressing the chimeric receptor containing the yeast Gal4-DNA

binding domain fused to the human PPARα- or PPARγ-LBD and the reporter plasmid for these

Gal4 chimeric receptors (pGal5TKpGL3) containing five repeats of the Gal4 response elements

upstream of a minimal thymidine kinase promoter that is adjacent to the luciferase gene were

described previously.[27]

Cell Culture and Transfections. Human hepatoblastoma cell line HepG2 (Interlab Cell Line

Collection, Genoa, Italy) was cultured in minimum essential medium (MEM) containing 10% heat-

inactivated fetal bovine serum, 100 U of penicillin G mL^{-1}, and 100 μg of streptomycin sulfate

mL^{-1} at 37 °C in a humidified atmosphere of 5% CO_2. For transactivation assays, 10^5 cells per well

were seeded in a 24-well plate and transfections were performed after 24 h with CAPHOS, a

calcium phosphate method, according to the manufacturer's guidelines. Cells were transfected with

expression plasmids encoding the fusion protein Gal4−PPARα-LBD or Gal4−PPARγ-LBD (30 ng),

pGal5TKpGL3 (100 ng), and pCMVβgal (250 ng). Four hours after transfection, cells were treated for 20 h with the indicated ligands in triplicate. For studies involving the covalent antagonist **7**, before incubation with PPARγ ligands LJ570 and rosiglitazone, cells were first pre-incubated with 5 μM **7** for 3 h. Luciferase activity in cell extracts was then determined by a luminometer (VICTOR[3] V Multilabel Plate Reader, PerkinElmer). β-Galactosidase activity was determined using ortho-nitro-phenyl-β-D-galactopyranoside as previously described.[47] All transfection experiments were repeated at least twice.

Co-regulator recruitment by Fluorescence Resonance Energy Transfer assay. Fluorescence resonance energy transfer assays to evaluate PGC1α recruitment were performed in 384-well plates in a final volume of 10 μl. A mixture of 8 ng of human PPARγ-ligand-binding domain, 0.8 ng of europium-labeled anti-His antibody (PerkinElmer Life Sciences), 86 ng of allophycocyanin-labeled streptavidin (PerkinElmer Life Sciences) and 8 ng of biotinylated peptide (PRIMM, Milano, Italia) in a FRET buffer containing 50 mM Tris (pH 7.5), 50 mM KCl, 1 mM DTT, and 0.1% fatty acid free BSA was prepared. LJ570 was added in 5-point dose response curve starting at 10 μM as the highest concentration. The reactions were equilibrated for 1 h at room temperature and then measured in an Envision multiplate reader (PerkinElmer Life Sciences) using 340 nm as excitation and 615 and 665 nm as emission wavelengths. The ratio between 665 (allophycocyanin signal) and 615 (europium signal) was used to evaluate the peptide recruitment on the receptor. The peptide sequence used for PGC-1α was Biotin-DGTPPPQEAEEPSLLKKLLLAPANT-COOH (NR box 1) spanning amino acids 130 –154 (reference no. NP_037393).

Cell Cultures. Hepa1-6 were cultured in DMEM supplemented by 10% fetal bovine serum and 1% penicillin-streptomycin at 37 °C in a humidified atmosphere of 5% CO_2. Cells were treated once with LJ570 or Wy-14,643. RNA was extracted 6 hours after treatments. Adipogenesis assays were performed as previously described.[36] Briefly, 3T3-L1 cells (ATCC) were cultured in DMEM

supplemented by 10% bovine calf serum; 2 days after reaching confluence, cells were differentiated in the presence of rosiglitazone or LJ570 at the indicated concentration and 5 μg insulin mL^{-1}. Culture medium was replenished with ligands three times every other day. Lipid accumulation was determined by staining cellular lipids with Oil Red O. Pictures were taken with an Axiovert 200 microscope (Zeiss) at 20X magnification. The quantification of the intracellular dye was performed after isopropanol extraction and spectrophotometric reading at 490 nm.

For experiments conducted with 10 μM LJ570, 2 days after reaching confluence, 3T3-L1 cells were differentiated with or without prior induction of adipocyte differentiation with the mixture 0.1 μM dexamethasone, 500 μM 3-isobutyl-1-methylxanthine, and 174.5 μM insulin. After 48 h, the medium was removed and replaced by DMEM containing 174.5 nM insulin with or without rosiglitazone (2 μM) or LJ570 (10 μM) and renewed every other day. Lipids contained in non-differentiated and differentiated cells were determined by staining cellular lipids with Oil Red O as reported above.[48]

RNA Extraction and Gene Expression Analysis. Gene expression analysis was performed as previously described.[36] Total RNA was extracted from Hepa1-6 and 3T3-L1 cells with TRIzol (Sigma), followed by purification on a Nucleospin RNA II column (Macherey Nagel, Germany) according to the manufacturer's instructions. Purified total RNA samples were quantified with Nanodrop (Thermo Scientific, Wilmington, DE). One μg of total RNA was used to quantitate mRNA levels of PPAR target genes by real-time qPCR using iScriptTM One Step RT-PCR for Probes (Bio-Rad) in a CFX 384 thermal cycler (Bio-Rad). 36B4 was used as housekeeping gene for data normalization.

In vitro kinase assay. The assay was performed on WT-PPARγ in the apo form and in the complex with LJ570 and rosiglitazone. For the kinase assay, stock solutions of ligands were prepared by diluting with 100% DMSO to a concentration of 50 mM. The stock solutions were further diluted

with 50 mM Tris HCl pH 7.5 up to the final concentrations of 0.1 μM, 1 μM and 10 μM respectively, and pre-equilibrated overnight at 4°C with the protein. Kinase assay was carried out at 30 °C for 3.5 h in 300 μL volume buffer containing 50 mM Tris HCl pH 7.5, 7.2 μg mL^{-1} PPARγ, 0.1-1-10 μM ligand, 25 mM MgCl$_2$, 50 μM DTT, 2 mM ATP, 0.66 ng mL^{-1} CDK5/p35 (Sigma Aldrich code n. SRP5011).

ELISA of PPARγ phosphorylation. Polystyrene microwell plates (Nunc immuno-plate Maxisorp 96 well, Sigma code M9410) were coated with the reaction mixture. After overnight incubation at 4°C, the coated wells were washed three times with WB (PBS + Tween 0.005%) and left to block in PBS containing 1% bovine serum for 90 min at 37 °C. The wells were then washed three times with WB and 100 μL of anti-phospho-Ser/The-Pro antibody (Sigma Aldrich code n. A05368) diluted 1:500 in PBS was added to the wells and incubated for 60 min at 37 °C. The wells were washed three times with WB and 100 μL of Anti-Mouse IgG (whole molecule)– Peroxidase antibody produced in goat (Sigma Aldrich code n. A4416) diluted 1:1000 in PBS were added to the wells. After 60 min of incubation at 37 °C, the wells were washed three times with WB and 200 μL of *o*-phenylenediamine dihydrochloride (Sigmafast OPD code n. P9187) dissolved in water were added to the wells. Optical density (OD) was measured at 450 nm using Apply Scan Thermofisher Reader and the data were processed using Excel.

2-Deoxy-D-glucose uptake assay. Glucose uptake activity of fully differentiated 3T3-L1 adipocytes was measured by the chemiluminescent assay[49] using Glucofax kit as described by the manufacturer (Yelen, Ensues la Redonne, France). To obtain differentiated adipocytes, 3T3-L1 cells were maintained two days at confluency then incubated for two days in the induction mixture (0.1 μM dexamethasone, 500 μM 3-isobutyl-1-methylxanthine, and 174.5 nM insulin). The induction

mixture was then replaced by DMEM containing 174.5 nM insulin. After 48 h, insulin was removed from the media and 48 h later cells were treated with LJ570 or rosiglitazone or both. Glucose uptake experiment was carried out 17 h later.

Statistical Analyses. Statistical analyses were performed via one-way analysis of variance with Dunnet or Bonferroni post-test analysis for multiple group comparisons using GraphPad Prism version 5.0 (GraphPad Software, San Diego, CA). Differences with p values ≤ 0.05 were considered statistically significant.

PPAR Protein Expression and Purification. PPARγ-LBD was expressed as N-terminal His-tagged proteins using a pET28 vector and then purified as previously described.[34] Briefly, freshly transformed *E. coli* BL21 DE3 were grown in LB medium with 30 μg of kanamycin mL^{-1} at 310 K to an OD of 0.6. The culture was then induced with 0.2 mM isopropyl-β-D-thio-galactopyranoside and further incubated at 291 K for 20 h. Cells were harvested and resuspended in a 20 mL L^{-1} culture of Buffer A (20 mM Tris, 150 mM NaCl, 10% glycerol, 1 mM Tris 2-carboxyethylphosphine HCl (TCEP), pH 8) in the presence of protease inhibitors (Complete Mini EDTA-free; Roche Applied Science). Cells were sonicated, and the soluble fraction was isolated by centrifugation (35,000 x g for 45 min). The supernatant was loaded onto a Ni^{2+}-nitrilotriacetic acid column (GE Healthcare) and eluted with a gradient of imidazole 0-500 mM in Buffer A (batch method). The pure protein was identified by SDS PAGE. The protein was then dialyzed over buffer A to remove imidazole, and it was cleaved with thrombin protease (GE Healthcare) (10 units mg^{-1}) at room temperature for 2 h. The digested mixture was reloaded onto a Ni^{2+}-nitriloacetic acid column to remove His tag and the undigested protein. The flow-through was dialyzed with buffer B (20 mM Tris, 10% glycerol, 1 mM TCEP, pH 8) to remove NaCl and then loaded onto a Q-Sepharose HP column (GE Healthcare) and eluted with a gradient of NaCl 0-500 mM in Buffer B

with a BioLogic DuoFlow FPLC system (Bio-Rad Laboratories, Italy). Finally, the proteins were purified by gel-filtration chromatography on a HiLoad Superdex 75 column (GE Healthcare) and eluted with Buffer C (20 mM Tris, 1 mM TCEP, 0.5 mM EDTA, pH 8). The proteins were then concentrated at 8.5 mg mL^{-1} using Amicon centrifugal concentrators with a 10 kDa cutoff membrane (Millipore, USA).

Crystallization and Data Collection. Crystals of apo-PPARγ were obtained by vapor diffusion at 18 °C using a sitting drop made by mixing 2 μL of protein solution with 2 μL of reservoir solution (0.8 M Na Citrate, 0.15 M Tris, pH 8.0). The crystals were soaked for four days in a storage solution (1.2 M Na Citrate, 0.15 M Tris, pH 8.0) containing the ligand LJ570 (0.2 mM). Other crystals of apo-PPARγ were soaked for two weeks in the same storage solution containing LJ570 (0.3 mM). The ligand dissolved in DMSO (50 mM) was diluted in the storage solution so that the final concentration of DMSO was 1%. The storage solution with glycerol 20% (v/v) was used as cryoprotectant. Crystals (0.1x0.1 mm) of PPARγ/LJ570 from the two different soaking conditions belong to the space group *C2* with cell parameters shown in Table 1 of Supporting Information.

Structure Determination and Refinement. X-ray data set from the two different soaking conditions were collected at 100 K under a nitrogen stream using sinchrotron radiation (beamline XRD1 at Elettra, Trieste, Italy and beamline ID29 at ESRF, Grenoble, France). The collected data were processed using the programs Mosflm and Scala.[50] Structure solution was performed with AMoRe,[51] using the coordinates of PPARγ/(*R*)-**1**[35] (PDB code 3D6D) as the starting model. The coordinates were then refined with CNS[52] including data between 48.0 and 2.5 Å, for the first data collection, and with PHENIX[53] including data between 57.9 and 2.0 Å, for the second collection (long-term soaking). The statistics of crystallographic data and refinement are summarized in Table 1 of Supporting Information. The coordinates and structure factors for the two PPARγ/LJ570

structures described here have been deposited in the PDB under accession number 4JL4 and 6F2L, respectively.

Computational Chemistry. Molecular modeling and graphics manipulations were performed using Maestro 11.3 (Maestro, Schrödinger, LLC, New York, NY, 2018) and UCSF-Chimera 1.8.1 (http://www.cgl.ucsf.edu/chimera) software packages, running on a E4 Computer Engineering E1080 workstation provided of an Intel Core i7-930 Quad-Core processor. GOLD 5.5 (CCDC Software Limited: Cambridge, U.K., 2008) was used for docking calculations.[54] Figures were generated using Pymol 2.0 (Schrödinger, LLC, New York, NY, 2017).

Modeling of PPARγ structure. The initial coordinates of PPARγ covalently-bound with **7** were taken from the X-ray crystal structure solved at 2.15 Å resolution (PDB ID 3B0R). As the coordinates of the highly flexible Ω-loop structure, comprising residues I262-S274, were not fully resolved, we refined this crystal structure computationally. To select the most suitable conformation of the Ω-loop for the protein model generation, we systematically scrutinized the PDB structures of PPARγ in complex with ligands occupying the alternate site. Our analysis included structures with PDB codes 3SZ1,[43a] 3K8S,[38] 5DWL, 5DV3,[43f] and 5GTO.[43e] Taking into account resolution, R-factor and completeness, the structure of PPARγ in complex with the partial agonist S35 (PDB code 5GTO) was selected as a template to build the Ω-loop. Then, the starting **7**-bound PPARγ crystal structure was modified by including the 12 missing residues from the 5GTO crystal structure. Insertion of the missing residues was carried out using the MODELLER interface in UCSF Chimera 1.6.1.[55] The obtained structure was energy-minimized for 2500 iterations utilizing the OPLS2005 force field and the Polak-Ribiere conjugate minimization scheme in Macromodel (MacroModel, Schrödinger, LLC, New York, NY, 2018.) in order to relieve structural inconsistencies in bond geometries.

Protein and Ligand Preparation. The constructed PPARγ model and the coordinates of PPARα in complex with the partial agonist AL29-26 determined at 1.83 Å resolution (PDB: 5HYK)[56] were processed through the Protein Preparation Wizard implemented in Maestro. All crystallographic water molecules and other chemical components were deleted, the right bond orders as well as charges and atom types were assigned, and the hydrogen atoms were added. Arginine and lysine side chains were considered as cationic at the guanidine and ammonium groups, and the aspartic and glutamic residues were considered as anionic at the carboxylate groups. The imidazole rings of H449 and H323 into PPARγ and of H440 into PPARα were set in their Nε2-H (N tau-H) tautomeric state. An exhaustive sampling of the orientations of groups, whose H-bonding network needs to be optimized, was performed. Finally, the protein structure was refined with a restrained minimization with the OPLS2005 force field by imposing a 0.3 Å root-mean-square deviation (rmsd) limit as the constraint.

The molecular structure of compound LJ570 was built using the fragment dictionary of Maestro and preprocessed with LigPrep (LigPrep, Schrödinger, LLC, New York, NY, 2018), which prepares the ligands in multiple protonation and tautomerization states at a neutral pH. The structure was then optimized by Macromodel 11.7 (Schrödinger, LLC, New York, NY, 2017, USA) using the MMFF force field with the steepest descent (1000 steps) followed by truncated Newton conjugate gradient (500 steps) methods. Partial atomic charges were computed using the OPLS-AA force field.

Docking Simulations. Molecular docking of LJ570 was performed by means of the GOLD software,[42] which uses a genetic algorithm for determining the docking modes of ligands and proteins. The region surrounded by helix H3 and the Ω loop between helices H2′ and H3 in PPARγ was chosen as binding site origin. The binding site radius was set equal to 15 Å. For docking in PPARα, the coordinates of the co-crystallized ligand AL29-26 were chosen as active-site origin. The active-site radius was set equal to 10 Å. Each GA run used the default parameters of 100000 genetic operations on an initial population of 100 members divided into five subpopulations, with

weights for crossover, mutation, and migration being set to 95, 95, and 10, respectively. GOLD allows a user-definable number of GA runs per ligand, each of which starts from a different orientation. For these experiments, the number of GA runs was set to 200 without the option of early termination and scoring of the docked poses was performed with the original ChemPLP scoring function followed by rescoring with ChemScore.[57] The final receptor–ligand complex was chosen interactively by selecting the highest scoring pose that was consistent with experimentally-derived information about the binding mode of the ligand.

Supporting Information

Statistics of crystallographic data and refinement, graphics of PPAR-target gene expression analysis and Oil Red O staining. Docking of LJ570 into PPARα binding pocket.

Molecular formula strings and the associated biological data (CSV file).

Accession Codes

PDB ID of PPARγ/LJ570: 4JL4 and 6F2L.

Authors will release the atomic coordinates and experimental data upon article publication.

Corresponding Author Information

*E-mail: fulvio.loiodice@uniba.it

Present/Current Author addresses

Marco Giudici

Post Doc Wallenberg Centre for Protein Research

School of Engineering Sciences in Chemistry, Biotechnology and Health

KTH | AlbaNova plan 3

SE-106 91, Stockholm (Sweden)

giudici@kth.se | kth.se

Author Contributions

Acknowledgment

Abbreviations Used

PPAR, peroxisome proliferator-activated receptor; LBD, ligand binding domain; TZDs, thiazolidinediones; SPPARM, selective peroxisome proliferator-activated receptor modulator; CDK5, cyclin-dependent kinase 5; PGC-1α, peroxisome proliferator-activated receptor gamma coactivator 1-alpha; FABP4, fatty acid binding protein 4; ADIPOQ, adiponectin; GLUT4, glucose transporter 4; CD36, class B scavenger receptor; PCK1, phosphoenolpyruvate carboxykinase 1, GK, glycerol kinase; IDH3a, isocitrate dehydrogenase subunit alpha; SUCLG1, succinyl-CoA ligase subunit alpha; ACOX1, acyl-Coenzyme A oxidase 1; CPT1a, carnitine palmitoyltransferase 1a; ACADM, acyl-Coenzyme A dehydrogenase, medium chain.

References

(1) Danaei, G.; Finucane, M. M.; Lu, Y.; Singh, G. M.; Cowan, M. J.; Paciorek, C. J.; Lin, J. K.; Farzadfar, F.; Khang, Y.-H.; Stevens, G. A.; Rao, M.; Ali, M. K.; Riley, L. M.; Robinson, C. A.; Ezzati, M.; Global burden of metabolic risk factors of chronic diseases collaborating group (blood glucose). National, regional, and global trends in fasting plasma glucose and diabetes prevalence since 1980: systematic analysis of health examination surveys and epidemiological studies with 370 country-years and 2–7 million participants. *Lancet* **2011**, *378*, 31–40.

2) Chapman, M. J.; Ginsberg, H. N.; Amarenco, P.; Andreotti, F.; Borén, J.; Catapano, A. L.; Descamps, O. S.; Fisher, E.; Kovanen, P. T.; Kuivenhoven, J. A.; Lesnik, P.; Masana, L.; Nordestgaard, B. G.; Ray, K. K.; Reiner, Z.; Taskinen, M. R.; Tokgözoglu, L.; Tybjærg-Hansen, A.; Watts, G. F. European atherosclerosis society consensus panel: triglyceride-rich lipoproteins and high-density lipoprotein cholesterol in patients at high risk of cardiovascular disease: evidence and guidance for management. *Eur. Heart J.* **201**1, *32*, 1345–1361.

3) Keech, A.; Simes, R. J.; Barter, P.; Best, J.; Scott, R.; Taskinen, M. R.; Forder, P.; Pillai, A.; Davis, T.; Glasziou, P.; Drury, P.; Kesäniemi, Y. A.; Sullivan, D.; Hunt, D.; Colman, P.; d'Emden, M.; Whiting, M.; Ehnholm, C.; Laakso, M. FIELD study investigators: Effects of long-term fenofibrate therapy on cardiovascular events in 9795 people with type 2 diabetes mellitus (the FIELD study): randomised controlled trial. *Lancet* **2005**, *366*, 1849–1861.

4) ACCORD Study Group, Ginsberg, H. N.; Elam, M. B.; Lovato, L. C.; Crouse, J. R. 3rd; Leiter, L. A.; Linz, P.; Friedewald, W. T.; Buse, J. B.; Gerstein, H. C.; Probstfield, J.; Grimm, R. H.; Ismail-Beigi, F.; Bigger, J. T.; Goff, D. C. Jr; Cushman, W. C.; Simons-Morton, D. G.; Byington, R. P. Effects of combination lipid therapy in type 2 diabetes mellitus. *N. Engl. J. Med.* **2010**, *362*,

1563–1574.

5) Fruchart, J.-C. Peroxisome proliferator-activated receptor-alpha (PPARalpha): at the crossroads of obesity, diabetes and cardiovascular disease. *Atherosclerosis* **2009**, *205*, 1–8.

6) Hottelart, C.; el Esper, N.; Achard, J. M.; Pruna, A.; Fournier, A. Fenofibrate increases blood creatinine, but does not change the glomerular filtration rate in patients with mild renal insufficiency. *Nephrologie* **1999**, *20*, 41–44.

7) Fruchart, J.-C. Selective peroxisome proliferator-activated receptor α modulators (SPPARMα): the next generation of peroxisome proliferator-activated receptor α agonists. *Cardiovasc. Diabetol*. **2013**, *12:82*.

8) Fruchart J.-C. Pemafibrate (K-877), a novel selective peroxisome proliferator-activated receptor alpha modulator for management of atherogenic dyslipidaemia. *Cardiovasc. Diabetol.* **2017**, *16:124*.

(9) Campbell, I. W. The clinical significance of PPAR gamma agonism. *Curr. Mol. Med.* **2005**, *5*, 349−363.

(10) Guan, Y.; Hao, C.; Cha, D. R.; Rao, R.; Lu, W.; Kohan, D. E.; Magnuson, M. A.; Redha, R.; Zhang, Y.; Breyer, M. D. Thiazolidinediones expand body fluid volume through PPARγ stimulation of ENaC-mediated renal salt absorption. *Nat. Med.* **2005**, *11*, 861–866.

(11) Home, P. D.; Pocock, S. J.; Beck-Nielsen, H.; Curtis, P. S.; Gomis, R.; Hanefeld, M.; Jones, N. P.; Komajda, M.; McMurray, J. J.; RECORD Study Team. Rosiglitazone evaluated for

cardiovascular outcomes in oral agent combination therapy for type 2 diabetes (RECORD). A multicentre, randomised, open-label trial. *Lancet* **2009**, *373*, 2125–2135.

(12) Shockley, K. R.; Lazarenko, O. P.; Czernik, P. J.; Rosen, C. J.; Churchill, G. A.; Lecka-Czernik, B. PPARγ2 nuclear receptor controls multiple regulatory pathways of osteoblast differentiation from marrow mesenchymal stem cells. *J. Cell. Biochem*. **2009**, *106*, 232–246.

(13) Wei, W.; Wang, X.; Yang, M.; Smith, L. C.; Dechow, P. C.; Sonoda, J.; Evans, R. M.; Wan, Y. PGC1α mediates PPARγ activation of osteoclastogenesis and rosiglitazone-induced bone loss. *Cell Metab.* **2010**, *11*, 503–516.

(14) Hansen, B. C.; Tigno, X. T.; Bénardeau, A.; Meyer, M.; Sebokova, E.; Mizrahi, J. Effects of aleglitazar, a balanced dual peroxisome proliferator-activated receptor α/γ agonist on glycemic and lipid parameters in a primate model of the metabolic syndrome. *Cardiovasc. Diabetol.* **2011**, *10*, 7.

(15) Lohray, B. B.; Lohray, V. B.; Bajji, A. C.; Kalchar, S.; Poondra, R. R.; Padakanti, S.; Chakrabarti, R.; Vikramadithyan, R. K.; Misra, P.; Juluri, S.; Mamidi, N. V.; Rajagopalan, R. (-)3-[4-[2-(Phenoxazin-10-yl)ethoxy]phenyl]-2-ethoxypropanoic acid [(-)DRF 2725]: a dual PPAR agonist with potent antihyperglycemic and lipid modulating activity. *J. Med. Chem.* **2001**, *44*, 2675–2678.

(16) Hegarty, B. D.; Furler, S. M.; Oakes, N. D.; Kraegen, E. W.; Cooney, G. J. Peroxisome proliferator-activated receptor (PPAR) activation induces tissue-specific effects on fatty acid uptake and metabolism in vivo - a study using the novel PPARalpha/gamma agonist tesaglitazar. *Endocrinology* **2004**, *145*, 3158–3164.

(17) Heald, M.; Cawthorne, M. A. Dual acting and pan-PPAR activators as potential anti-diabetic therapies. *Handb. Exp. Pharmacol.* **2011**, *203*, 35–51.

(18) Lecka-Czernik, B. Aleglitazar, a dual PPARα and PPARγ agonist for the potential oral treatment of type 2 diabetes mellitus. IDrugs **2010**, *13*, 793–801.

(19) Jeong, H. W.; Lee, J. W.; Kim, W. S.; Choe, S. S.; Kim, K. H.; Park, H. S.; Shin, H. J.; Lee, G. Y.; Shin, D.; Lee, H.; Lee, J. H.; Choi, E. B.; Lee, H. K.; Chung, H.; Park, S. B.; Park, K. S.; Kim, H. S.; Ro, S.; Kim, J. B. A newly identified CG301269 improves lipid and glucose metabolism without body weight gain through activation of peroxisome proliferator-activated receptor alpha and gamma. *Diabetes* **2011**, *60*, 496–506.

(20) Agrawal, R. The first approved agent in the glitazar's class: saroglitazar. *Curr. Drug Targets* **2014**, *15*, 151–155.

(21) Choi, J. H.; Banks, A. S.; Estall, J. L.; Kajimura, S.; Boström, P.; Laznik, D.; Ruas, J. L.; Chalmers, M. J.; Kamenecka, T. M.; Blüher, M.; Griffin, P. R.; Spiegelman, B. M. Anti-diabetic drugs inhibit obesity-linked phosphorylation of PPARγ by Cdk5. *Nature* **2010**, *466*, 451–456.

(22) Choi, J. H.; Banks, A. S.; Kamenecka, T. M.; Busby, S. A.; Chalmers, M. J.; Kumar, N.; Kuruvilla, D. S.; Shin, Y.; He, Y.; Bruning, J. B.; Marciano, D. P.; Cameron, M. D.; Laznik, D.; Jurczak, M. J.; Schürer, S. C.; Vidovi, D.; Shulman, G. I.; Spiegelman, B. M.; Griffin, P. R. Antidiabetic actions of a non-agonist PPARγ ligand blocking Cdk5-mediated phosphorylation. *Nature* **2011**, *477*, 477–481.

(23) Amato, A. A.; Rajagopalan, S.; Lin, J. Z.; Carvalho, B. M.; Figueira, A. C.; Lu, J.; Ayers, S. D.; Mottin, M.; Silveira, R. L.; Souza, P. C.; Mourão, R. H.; Saad, M. J.; Togashi, M.; Simeoni, L. A.; Abdalla, D. S.; Skaf, M. S.; Polikparpov, I.; Lima, M. C.; Galdino, S. L.; Brennan, R. G.; Baxter, J. D.; Pitta, I. R.; Webb, P.; Phillips, K. J.; Neves, F. A. GQ-16, a novel peroxisome proliferator-activated receptor γ (PPARγ) ligand, promotes insulin sensitization without weight gain. *J. Biol. Chem.* **2012**, *287*, 28169–28179.

(24) de Groot, J. C.; Weidner, C.; Krausze, J.; Kawamoto, K.; Schroeder, F. C.; Sauer, S.; Büssow, K. Structural characterization of amorfrutins bound to the peroxisome proliferator-activated receptor γ. *J. Med. Chem.* **2013**, *56*, 1535–1543.

(25) Pochetti, G.; Mitro, N.; Lavecchia, A.; Gilardi, F.; Besker, N.; Scotti, E.; Aschi, M.; Re, N.; Fracchiolla, G.; Laghezza, A.; Tortorella, P.; Montanari, R.; Novellino, E.; Mazza, F.; Crestani, M.; Loiodice, F. Structural insight into peroxisome proliferator-activated receptor γ binding of two ureidofibrate-like enantiomers by molecular dynamics, cofactor interaction analysis, and site-directed mutagenesis. *J. Med. Chem.* **2010**, *53*, 4354–4366.

(26) Laghezza, A.; Montanari, R.; Lavecchia, A.; Piemontese, L.; Pochetti, G.; Iacobazzi, V.; Infantino, V.; Capelli, D.; De Bellis, M.; Liantonio, A.; Pierno, S.; Tortorella, P.; Conte Camerino, D.; Loiodice, F. On the metabolically active form of metaglidasen: improved synthesis and investigation of its peculiar activity on peroxisome proliferator-activated receptors and skeletal muscles. *ChemMedChem* **2015**, *10*, 555–565.

(27) Pinelli, A.; Godio, C.; Laghezza, A.; Mitro, N.; Fracchiolla, G.; Tortorella, V.; Lavecchia, A.; Novellino, E.; Fruchart, J.-C.; Staels, B.; Crestani, M.; Loiodice, F. Synthesis, biological

evaluation, and molecular modeling investigation of new chiral fibrates with PPARalpha and PPARgamma agonist activity. *J. Med. Chem.* **2005**, *48*, 5509–5519.

(28) Fracchiolla, G.; Laghezza, A.; Piemontese, L.; Parente, M.; Lavecchia, A.; Pochetti, G.; Montanari, R.; Di Giovanni, C.; Carbonara, G.; Tortorella, P.; Novellino, E.; Loiodice, F. Synthesis, biological evaluation and molecular investigation of fluorinated peroxisome proliferator-activated receptors α/ γ dual agonists. *Bioorg. Med. Chem.* **2012**, *20*, 2141–2151.

(29) Fracchiolla, G.; Laghezza, A.; Piemontese, L.; Carbonara, G.; Lavecchia, A.; Tortorella, P.; Crestani, M.; Novellino, E.; Loiodice, F. Synthesis, biological evaluation, and molecular modeling investigation of chiral phenoxyacetic acid analogues with PPARalpha and PPARgamma agonist. *ChemMedChem* **2007**, *2*, 641–654.

(30) Laghezza, A.; Pochetti, G.; Lavecchia, A.; Fracchiolla, G.; Faliti, S.; Piemontese, L.; Di Giovanni, C.; Iacobazzi, V.; Infantino, V.; Montanari, R.; Capelli, D.; Tortorella, P.; Loiodice, F. New 2-(aryloxy)-3-phenylpropanoic acids as peroxisome proliferator-activated receptor α/γ dual agonists able to upregulate mitochondrial carnitine shuttle system gene expression. *J. Med. Chem.* **2013**, *56*, 60–72.

(31) Porcelli, L.; Gilardi, F.; Laghezza, A.; Piemontese, L.; Mitro, N.; Azzariti, A.; Altieri, F.; Cervoni, L.; Fracchiolla, G.; Giudici, M.; Guerrini, U.; Lavecchia, A.; Montanari, R.; Di Giovanni, C.; Paradiso, A.; Pochetti, G.; Simone, G. M.; Tortorella, P.; Crestani, M.; Loiodice, F. Synthesis, characterization and biological evaluation of ureidofibrate-like derivatives endowed with peroxisome proliferator-activated receptor activity. *J. Med. Chem.* **2012**, *55*, 37–54.

(32) Fracchiolla, G.; Laghezza, A.; Piemontese, L.; Tortorella, P.; Mazza, F.; Montanari, R.;

Pochetti, G.; Lavecchia, A.; Novellino, E.; Pierno, S.; Conte Camerino, D.; Loiodice, F. New 2-aryloxy-3-phenyl-propanoic acids as peroxisome proliferator-activated receptors alpha/gamma dual agonists with improved potency and reduced adverse effects on skeletal muscle function. *J. Med. Chem.* **2009**, *52*, 6382–6393.

(33) Fracchiolla, G.; Lavecchia, A.; Laghezza, A.; Piemontese, L.; Trisolini, R.; Carbonara, G.; Tortorella, P.; Novellino, E.; Loiodice, F. Synthesis, biological evaluation, and molecular modeling investigation of chiral 2-(4-chloro-phenoxy)-3-phenyl-propanoic acid derivatives with PPARalpha and PPARgamma agonist activity. *Bioorg. Med. Chem.* **2008**, *16*, 9498–9510.

(34) Pochetti, G.; Godio, C.; Mitro, N.; Caruso, D.; Galmozzi, A.; Scurati, S.; Loiodice, F.; Fracchiolla, G.; Tortorella, P.; Laghezza, A.; Lavecchia, A.; Novellino, E.; Mazza, F.; Crestani, M. Insights into the mechanism of partial agonism: crystal structures of the peroxisome proliferator-activated receptor gamma ligand-binding domain in the complex with two enantiomeric ligands. *J. Biol. Chem.* **2007**, *282*, 17314–17324.

(35) Montanari, R.; Saccoccia, F.; Scotti, E.; Crestani, M.; Godio, C.; Gilardi, F.; Loiodice, F.; Fracchiolla, G.; Laghezza, A.; Tortorella, P.; Lavecchia, A.; Novellino, E.; Mazza, F.; Aschi, M.; Pochetti, G. Crystal structure of the peroxisome proliferator-activated receptor gamma (PPARgamma) ligand binding domain complexed with a novel partial agonist: a new region of the hydrophobic pocket could be exploited for drug design. *J. Med. Chem.* **2008**, *51*, 7768–7776.

(36) Gilardi, F.; Giudici, M.; Mitro, N.; Maschi, O.; Guerrini, U.; Rando, G.; Maggi, A.; Cermenati, G.; Laghezza, A.; Loiodice, F.; Pochetti, G.; Lavecchia, A.; Caruso, D.; De Fabiani, E.; Bamberg, K.; Crestani, M. LT175 is a novel PPARα/γ ligand with potent insulin sensitizing effects and reduced adipogenic properties. *J. Biol. Chem.* **2014**, *289*, 6908–6920.

(37) Winitz, M.; Bloch-Frankenthal, L.; Izumiya, N.; Birnbaum, S. M.; Baker, C. G.; Greenstein, J. P. Studies on diastereoisomeric α-amino acids and corresponding α-hydroxy acids. VII. Influence of β-configuration on enzymic susceptibility. *J. Am. Chem. Soc.* **1956**, *78*, 2423–2430 and references therein.

(38) Li, Y.; Wang, Z.; Furukawa, N.; Escaron, P.; Weiszmann, J.; Lee, G.; Lindstrom, M.; Liu, J.; Liu, X.; Xu, H.; Plotnikova, O.; Prasad, V.; Walker, N.; Learned, R. M.; Chen J.-L. T2384, a novel antidiabetic agent with unique peroxisome proliferator-activated receptor γ binding properties. *J. Biol. Chem.* **2008**, *283*, 9168–9176.

(39) Hughes, T. S.; Shang, J.; Brust, R.; de Vera, I. M. S.; Fuhrmann, J.; Ruiz, C.; Cameron, M. D.; Kamenecka, T. M.; Kojetin D. J. Probing the complex binding modes of the PPARγ partial agonist 2- chloro- N- (3-chloro-4-((5-chlorobenzo[d]thiazol-2-yl)thio)phenyl)-4-(trifluoromethyl)benzene-sulfonamide (T2384) to orthosteric and allosteric sites with NMR spectroscopy. *J. Med. Chem.* **2016**, *59*, 10335−10341.

(40) a) Hughes, T. S.; Giri, P. K.; de Vera, I. M.; Marciano, D. P.; Kuruvilla, D. S.; Shin, Y.; Blayo, A. L.; Kamenecka, T. M.; Burris, T. P.; Griffin, P. R.; Kojetin, D. J. An alternate binding site for PPARγ ligands. *Nat. Commun.* **2014**, *5*, 3571; b) Brust, R.; Lin, H.; Fuhrmann, J.; Asteian, A.; Kamenecka, T. M.; Kojetin D. J. Modification of the orthosteric PPARγ covalent antagonist scaffold yields an improved dual-site allosteric inhibitor. *ACS Chem. Biol.* **2017**, *12*, 969−978.

(41) Leesnitzer, L. M.; Parks, D. J.; Bledsoe, R. K.; Cobb, J. E.; Collins, J. L.; Consler, T. G.; Davis, R. G.; Hull-Ryde, E. A.; Lenhard, J. M.; Patel, L.; Plunket, K. D.; Shenk, J. L.; Stimmel, J. B.; Therapontos, C.; Willson, T. M.; Blanchard, S. G. Functional consequences of cysteine

modification in the ligand binding sites of peroxisome proliferator activated receptors by GW9662. *Biochemistry* **2002**, *41*, 6640−6650.

(42) Jones, G.; Willett, P.; Glen, R. C.; Leach, A. R.; Taylor, R. Development and validation of a genetic algorithm for flexible docking. *J. Mol. Biol.* **1997**, *267*, 727–748.

(43) a) Puhl, A. C.; Bernardes, A.; Silveira, R. L.; Yuan, J.; Campos, J. L.; Saidemberg, D. M.; Palma, M. S.; Cvoro, A.; Ayers, S. D.; Webb, P.; Reinach, P. S.; Skaf, M. S.; Polikarpov, I. Mode of peroxisome proliferator-activated receptor gamma activation by luteolin. *Mol. Pharmacol.* **2012**, *81*, 788–799; b) Waku, T.; Shiraki, T.; Oyama, T.; Fujimoto, Y.; Maebara, K.; Kamiya, N.; Jingami, H.; Morikawa, K. Structural insight into PPARgamma activation through covalent modification with endogenous fatty acids. *J. Mol. Biol.* **2009**, *385*, 188–199; c) Waku, T.; Shiraki, T.; Oyama, T.; Morikawa, K. Atomic structure of mutant PPARgamma LBD complexed with 15d-PGJ2: novel modulation mechanism of PPARgamma/RXRalpha function by covalently bound ligands. *FEBS lett*. **2009**, *583*, 320–4; d) Vasaturo, M.; Fiengo, L.; De Tommasi, N.; Sabatino, L.; Ziccardi, P.; Colantuoni, V.; Bruno, M.; Cerchia, C.; Novellino, E.; Lupo, A.; Lavecchia, A.; Dal Piaz, F. A compound-based proteomic approach discloses 15-ketoatractyligenin methyl ester as a new PPARgamma partial agonist with antiproliferative ability. *Sci. Rep.* **2017**, *7*, 41273; e) Jang, J. Y.; Koh, M.; Bae, H.; An, D. R.; Im, H. N.; Kim, H. S.; Yoon, J. Y.; Yoon, H. J.; Han, B. W.; Park, S. B.; Suh, S. W. Structural basis for differential activities of enantiomeric PPARγ agonists: binding of S35 to the alternate site. *Biochim. Biophys. Acta* **2017**, *1865*, 674–681; f) Bae, H.; Jang, J. Y.; Choi, S.-S.; Lee, J.-J.; Kim, H.; Jo, A.; Lee, K.-J.; Choi, J. C.; Suh, S. W.; Park, S. B. Mechanistic elucidation guided by covalent inhibitors for the development of anti-diabetic PPARγ ligands. *Chem. Sci.* **2016**, *7*, 5523–5529.

(44) Mottin, M.; Souza, P. C.; Skaf, M. S. Molecular recognition of PPARγ by kinase CDK5/p25:

insights from a combination of protein–protein docking and adaptive biasing force simulations. The *J. Phys. Chem. B* **2015**, *119*, 8330–8339.

(45) Shang, J.; Brust, R.; Mosure, S. A.; Bass, J.; Munoz-Tello, P.; Lin, H.; Hughes, T. S.; Tang, M.; Ge, Q.; Kamenecka, T. M.; Kojetin, D. J. Coincident binding of synthetic and natural ligands to the nuclear receptor PPARγ. *bioRxiv* **2018**, 252817.

(46) Mukherjee, R.; Hoener, P. A.; Jow, L.; Bilakovics, J.; Klausing, K.; Mais, D. E.; Faulkner, A.; Croston, G. E.; Paterniti, J. R. Jr. A selective peroxisome proliferator-activated receptor-γ (PPARγ) modulator blocks adipocyte differentiation but stimulates glucose uptake in 3T3–L1 adipocytes. *Mol. Endocrino*l. **2000**, *14*, 1425–1433.

(47) Hollon, T.; Yoshimura, F. K. Variation in enzymatic transient gene expression assays. *Anal. Biochem.* **1989**, *182*, 411−418.

(48) Brusotti, G.; Montanari, R.; Capelli, D.; Cattaneo, G.; Laghezza, A.; Tortorella, P.; Loiodice, F.; Peiretti, F.; Bonardo, B.; Paiardini, A.; Calleri, E.; Pochetti, G. Betulinic acid is a PPARγ antagonist that improves glucose uptake, promotes osteogenesis and inhibits adipogenesis. *Sci. Rep.* **2017**, *7*, 5777.

(49) Vidal, N.; Cavaillé, J. P.; Poggi, M.; Peiretti, F. A non-radioisotope chemiluminescent assay for evaluation of 2-deoxyglucose uptake in 3T3-L1 adipocytes. Effect of various carbonyls species on insulin action. *Biochimie* **2012**, *94*, 2569–2576.

(50) Kabsch, W. Xds. *Acta Crystallogr. D Biol. Crystallogr.* **2010**, *66*, 125–132.

(51) Navaza, J. AMoRe: an automated package for molecular replacement. *Acta Crystallogr.* **1994**, *A50*, 157–163.

(52) Brünger, A. T.; Adams, P. D.; Clore, G. M.; DeLano, W. L.; Gros, P.; Grosse-Kunstleve, R. W.; Jiang, J. S.; Kuszewski, J.; Nilges, M.; Pannu, N. S.; Read, R. J.; Rice, L. M.; Simonson, T.; Warren, G. L. Crystallography & NMR system: a new software suite for macromolecular structure determination. *Acta Crystallogr. D Biol. Crystallogr.* **1998**, *54*, 905–921.

(53) Adams, P. D.; Afonine, P. V.; Bunkóczi, G.; Chen, V. B.; Davis, I. W.; Echols, N.; Headd, J. J.; Hung, L.-W.; Kapral, G. J.; Grosse-Kunstleve, R. W.; McCoy, A. J.; Moriarty, N. W.; Oeffner, R.; Read, R. J.; Richardson, D. C.; Richardson, J. S.; Terwilliger, T. C.; Zwart, P. H. PHENIX: a comprehensive Python-based system for macromolecular structure solution. *Acta Crystallogr. D Biol. Crystallogr.* **2010**, *66*, 213–221.

(54) Jones, G.; Willett, P.; Glen, R. C.; Leach, A. R.; Taylor, R. Development and validation of a genetic algorithm for flexible docking. *J. Mol. Biol.* 267, **1997**, *267*, 727–748.

(55) Yang, Z.; Lasker, K.; Schneidman-Duhovny, D.; Webb, B.; Huang, C. C.; Pettersen, E. F.; Goddard, T. D.; Meng, E. C.; Sali, A.; Ferrin, T. E. UCSF Chimera, MODELLER, and IMP: an integrated modeling system. *J. Struct. Biol.* **2012**, *179*, 269– 278.

(56) Capelli, D.; Cerchia, C.; Montanari, R.; Loiodice, F.; Tortorella, P.; Laghezza, A.; Cervoni, L.; Pochetti, G.; Lavecchia, A. Structural basis for PPAR partial or full activation revealed by a novel ligand binding mode. *Sci. Rep.* **2016**, *6*, 34792.

(57) Verdonk, M. L.; Cole, J. C.; Hartshorn, M. J.; Murray, C. W.; Taylor, R. D. Improved protein-

ligand docking using GOLD. *Proteins: Struct., Funct., Genet.* **2003**, *52*, 609– 623.

Table 1. Activity of the tested compounds in cell-based transactivation assay.

Cmp	PPARα		PPARγ	
	EC$_{50}$ (μM)	Emax[a]	EC$_{50}$ (μM)	Emax[a]
(S^I,S^{II})-**3**	5.9±0.6	47±3	9.8±1.2	61±5
(S^I,R^{II})-**3**	27±7	13±1	18±3	37±1
(R^I,S^{II})-**3**	9.5±2.5	4±1	25±2	27±1
(R^I,R^{II})-**3**	na	na	15±4	8±1
(*R*)-**6**	2.6±0.3	25±1	0.89±0.16	54±7
(*S*)-**6**	1.05±0.03	68±8	0.12±0.04	57±8
(*S*)-**1**	0.19±0.04	116±4	0.55±0.12	62±7
Wy-14,643	1.56±0.30	100±10	-	-
Rosiglitazone	-	-	0.039±0.003	100±9

[a]Efficacy values were calculated as a percentage of the maximum obtained fold induction with the reference compounds. na = not active.

FIGURE LEGENDS.

Figure 1. *(Left)* Chemical structure of the reference compounds (*S*)-**1** and (*R*)-**1** of the present study. *(Right)* Superposition of (*S*)-**1** (yellow) and (*R*)-**1** (green) in the PPARγ-LBD (gray).

Figure 2. Chemical structure of the compounds of the present study. The asterisks indicate the presence of two stereogenic centres for compounds **3** and **4** (*I*, *II*), whereas **5** has only one stereogenic centre.

Figure 3. Maximum effect of racemates **2-6** on activation of PPARα and PPARγ at concentrations increasing up to 100 μM in comparison with reference compounds Wy-14,643 (10 μM), rosiglitazone (2 μM), or (*S*)-**1** (25 μM).

Figure 4. Binding mode of (A) LJ570 (short-time soaking, yellow, PDB ID: 4JL4), (B) LJ570 (long-time soaking, cyan, PDB ID: 6F2L), and their superposition (C) with the antagonist **7** (purple), in the PPARγ-LBD (gray).

Figure 5. LJ570 does not induce lipid accumulation in 3T3-L1 mouse adipocytes. *A*, representative images of 3T3-L1 mouse preadipocytes differentiated in the presence of the indicated PPAR ligands. Cells were stained with Oil Red O, and pictures were taken with an Axiovert 200 microscope at 20X magnification. *Scale bar* = 40 μm. *Ctrl*, undifferentiated cells; *Ins*, undifferentiated cells treated with 5 μg of insulin/mL; *Rosiglitazone*, cells differentiated in the presence of 5 μg of insulin/mL and 5 μM Rosiglitazone; *LJ570*, cells differentiated in the presence of 5 μg of insulin/mL and 0.1 – 1 – 2.5 μM LJ570. *B*, spectrophotometric quantification of lipid content after solvent extraction of Oil Red O from 3T3-L1 mouse adipocytes differentiated in the

presence of the indicated treatments. ***, $p \leq 0.001$ *vs* Ins. Data are mean $\pm$ S.E. of triplicate samples.

Figure 6. LJ570 induces PGC1α recruitment on PPARγ and shows a synergistic effect with rosiglitazone. *(Insert)* The interaction of the PGC1α coactivator peptide with PPARγ in the presence of increasing concentrations of LJ570 was evaluated by FRET assays. The interaction was evaluated also in combination with three different concentrations (0.37 μM, 1 μM, 10 μM) of rosiglitazone. At these concentrations, the data for PGC1α coactivator recruitment by rosiglitazone alone correspond to those obtained in the presence of 0.1 microM LJ570, that is, about 100% compared to the experiments conducted with no ligand. In fact, as shown in the insert, LJ570 is inactive at 0.1 microM, therefore the recruitment of PGC1α can be considered as induced by rosiglitazone alone. The curve is expressed as the ratio of fluorescence reading at 665 and 615 nm multiplied by 10,000 and represents the mean $\pm$ S.E. of triplicate for each concentration of the ligand. Error bars do not show up on several data points because of very low standard deviations.

Figure 7. Luciferase reporter assay showing the concentration-dependent effects of (A) LJ570 and (B) rosiglitazone on PPARγ transactivation without **7** pretreatment (full line) and with **7** pretreatment (dotted line).

Figure 8. (A) Binding mode of LJ570 (aquamarine sticks) into the **7**-bound PPARγ LBD represented as a gray ribbon model. The covalent antagonist **7** is shown as magenta sticks. Only amino acids located within 4 Å of the bound ligand are displayed (white sticks) and labelled. The Ω-loop and the β-sheet region of the LBD are displayed. H-bonds discussed in the text are depicted as dashed deepblue lines. (B) The canonical site, which is completely enclosed within the alpha helical sandwich fold of the LBD, can accomodate LJ570 (magenta and yellow sticks representing different crystallized binding modes; PDB codes 6F2L and 4JL4). LJ570 (cyan sticks) can also bind

to a solvent accessible alternate site distinct from the canonical site, structurally defined as the region between H3 and the flexible Ω-loop. (C) LJ570 overlaps with the crystallized binding mode of SR1664 (orange sticks, PDB code: 5DWL) and S35 (limegreen sticks, PDB code: 5GTO) bound to the alternate site of the PPARγ-LBD. (D) LJ570 overlaps with the crystallized binding mode of nonanoic acid bound to the alternate site (yellow sticks, PDB code: 5UGM).

Figure 9. Percentage of S273 phosphorylation in the presence of 0.1, 1 and 10 μM LJ570 (rosiglitazone has been used as reference compound). PPAR+ is the positive control without ligand and PPAR- the negative control without Cdk5/p25. $**p \leq 0.01$; $*p \leq 0.05$. The experiments were performed in triplicate.

Figure 10. Cellular glucose uptake. (A) Cellular glucose uptake rate upon exposure to LJ570. Differentiated adipocytes were treated with the indicated concentrations of LJ570 for 17 h prior to insulin stimulation (+ insulin, 100 nM), then cellular glucose uptake was determined. Values are means ± SD expressed as fold relative to the untreated control. $****p < 0.0001$. (B) Differentiated adipocytes were treated with LJ570 (10 μM) and/or rosiglitazone (Rosi; 0.3 μM) for 17 h prior to insulin stimulation (+ insulin, 100 nM), then cellular glucose uptake was determined. Values are means ± SD expressed as fold relative to the untreated control. Letters a, b and c indicate significant differences (at least $p < 0.05$; one-way ANOVA followed by Bonferroni's post-hoc test) vs insuline alone, insuline + LJ570 and insulin + Rosi treatments, respectively.

Figure 1.

(S)-**1**. R = H; R' = CH₂Ph

(R)-**1**. R = CH₂Ph; R' = H

Figure 2.

2

3. R = CH₂Ph
4. R = CH₃
5. R = H

I

II

6
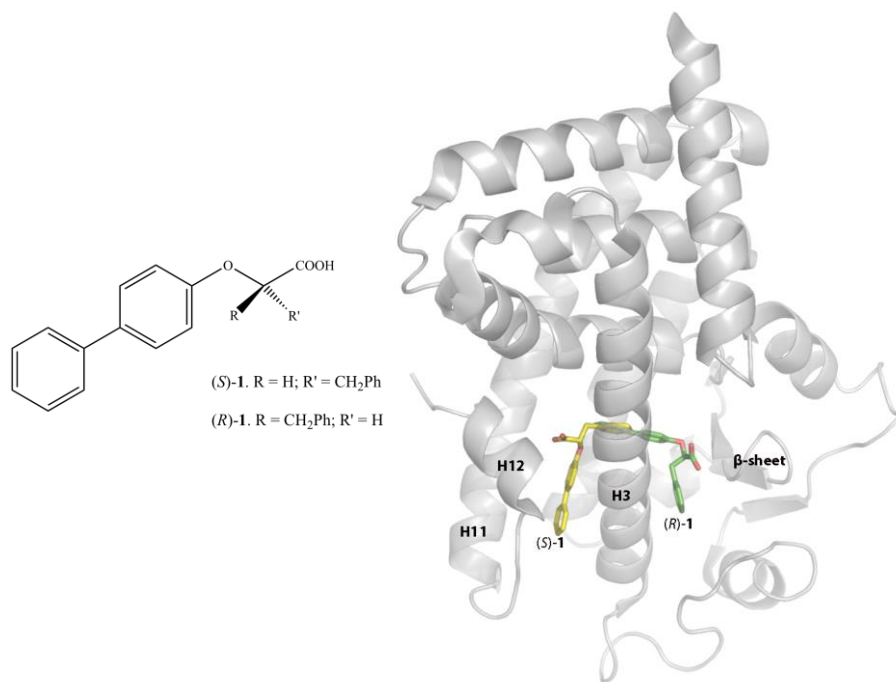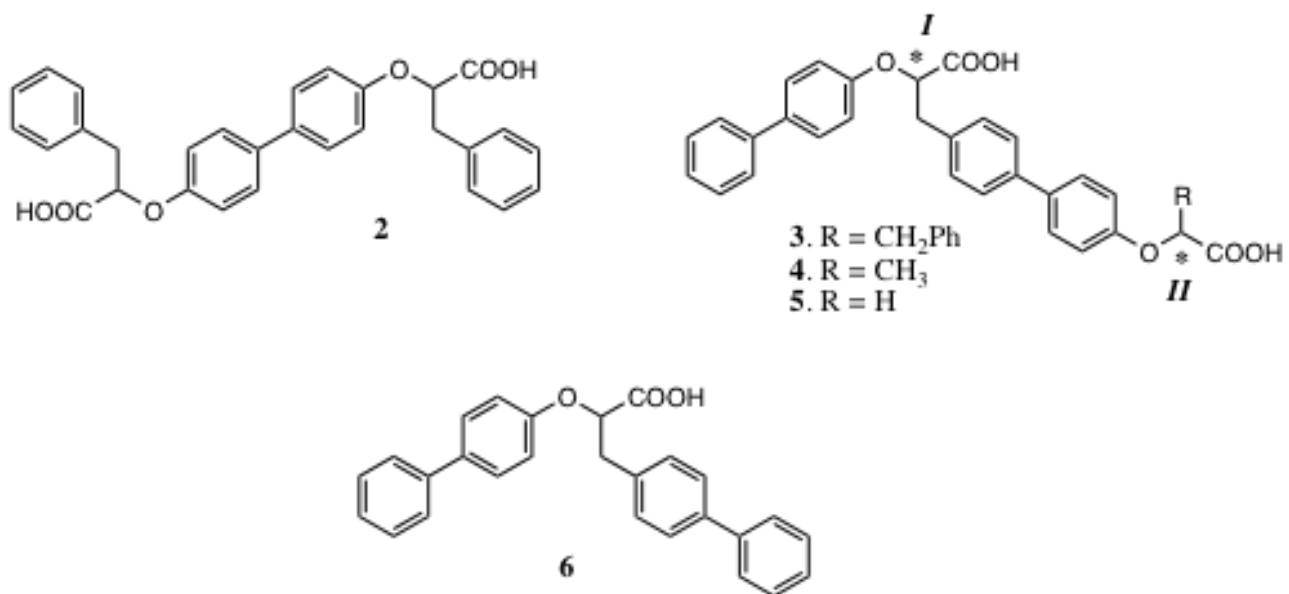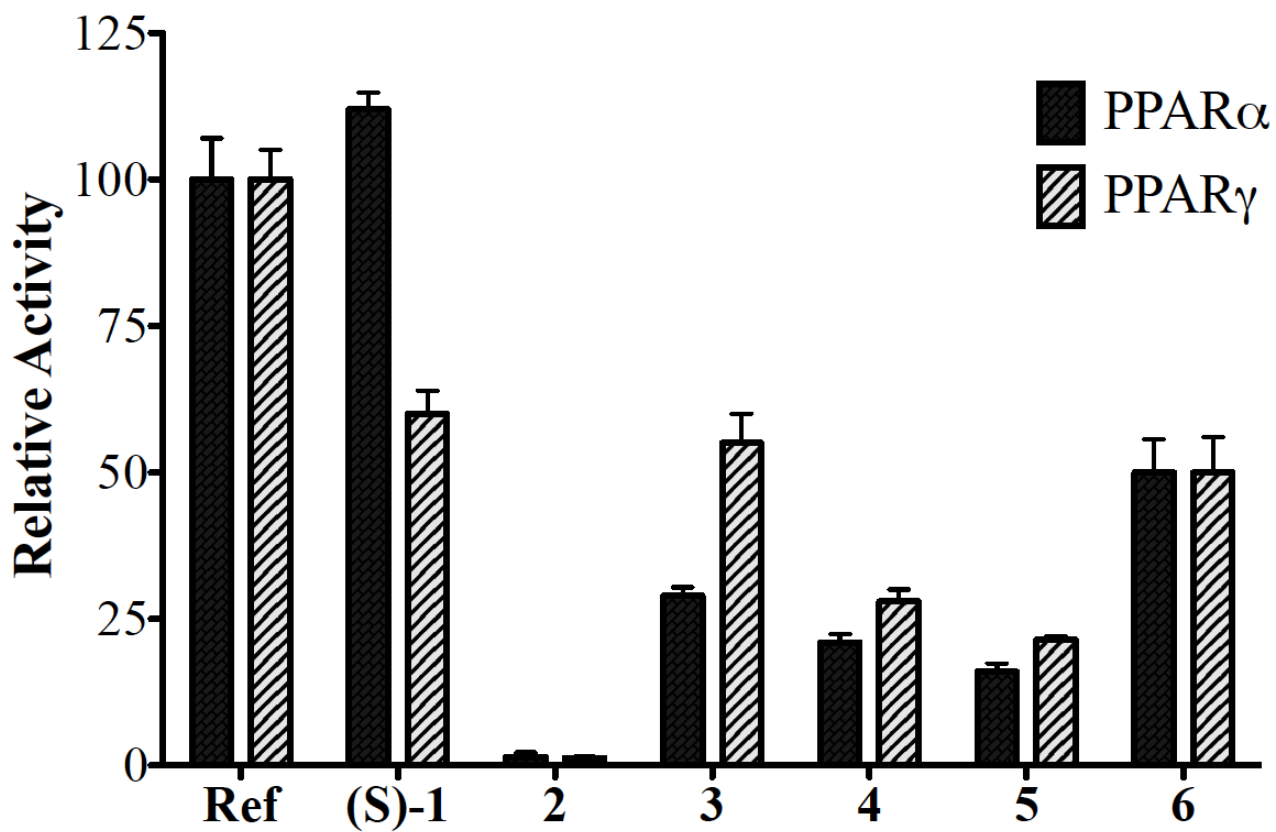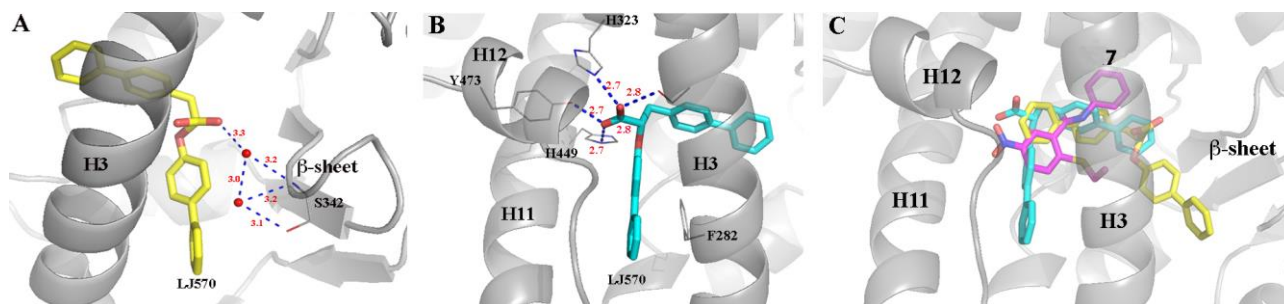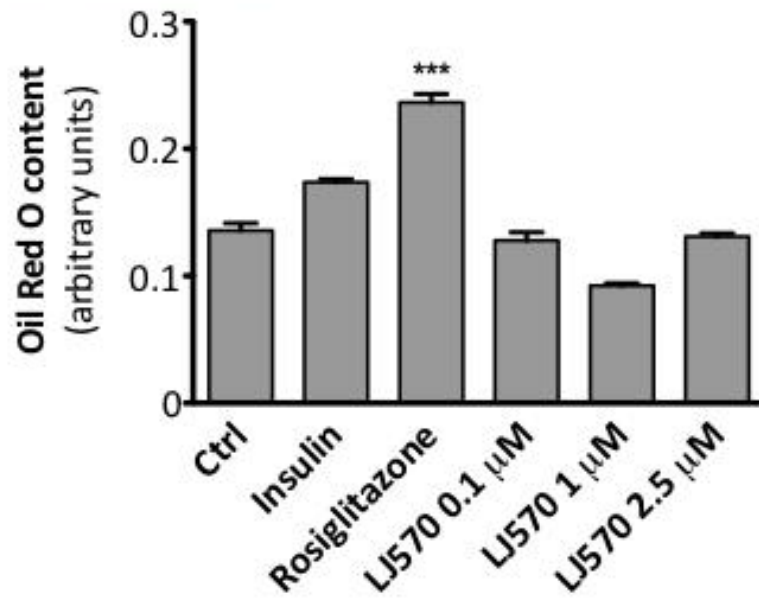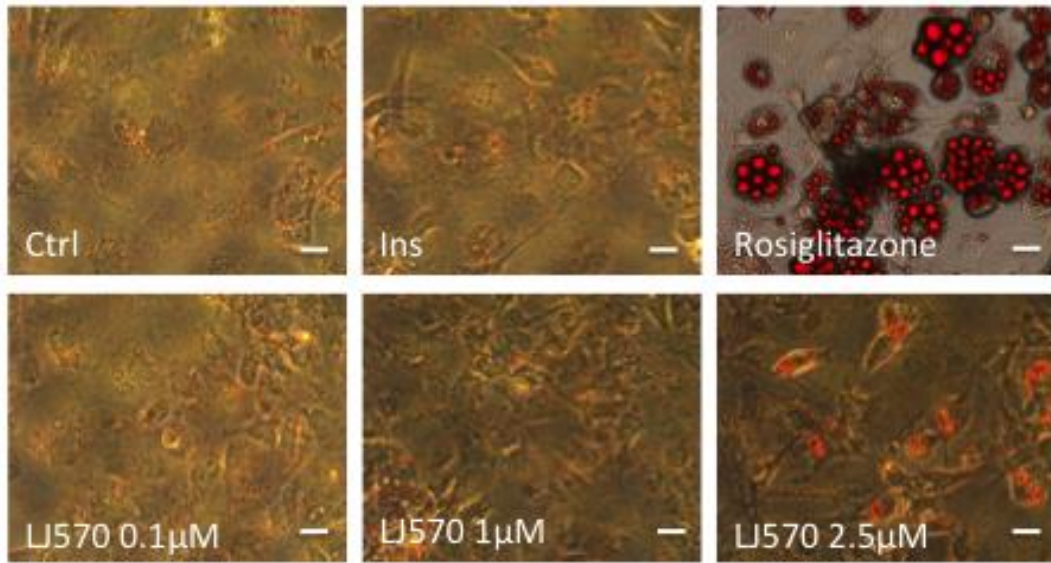
Figure 3.

Figure 4.

Figure 5.
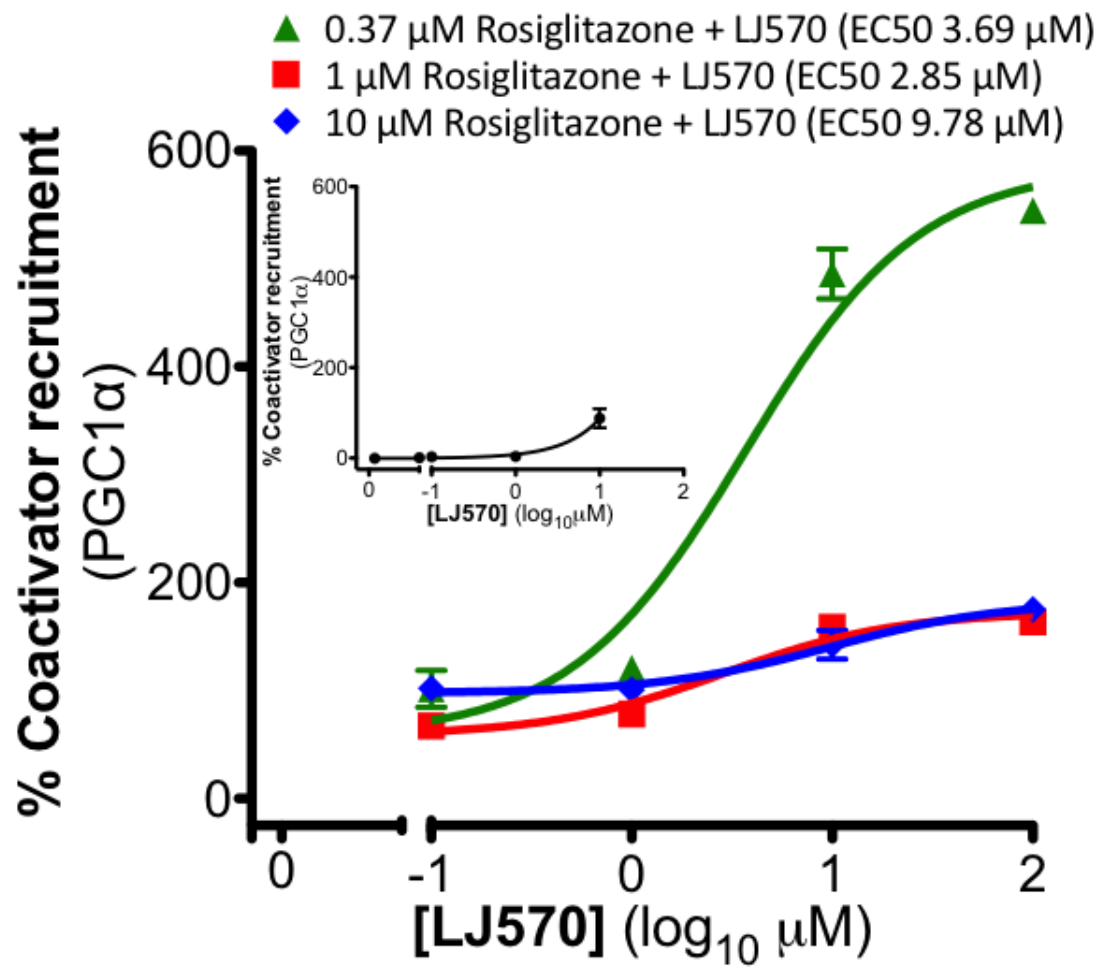
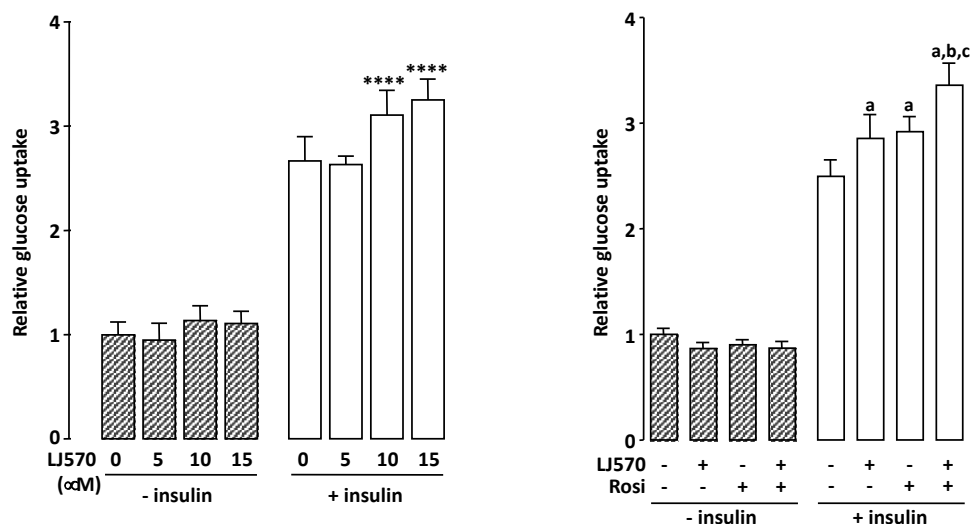**Figure 6.**
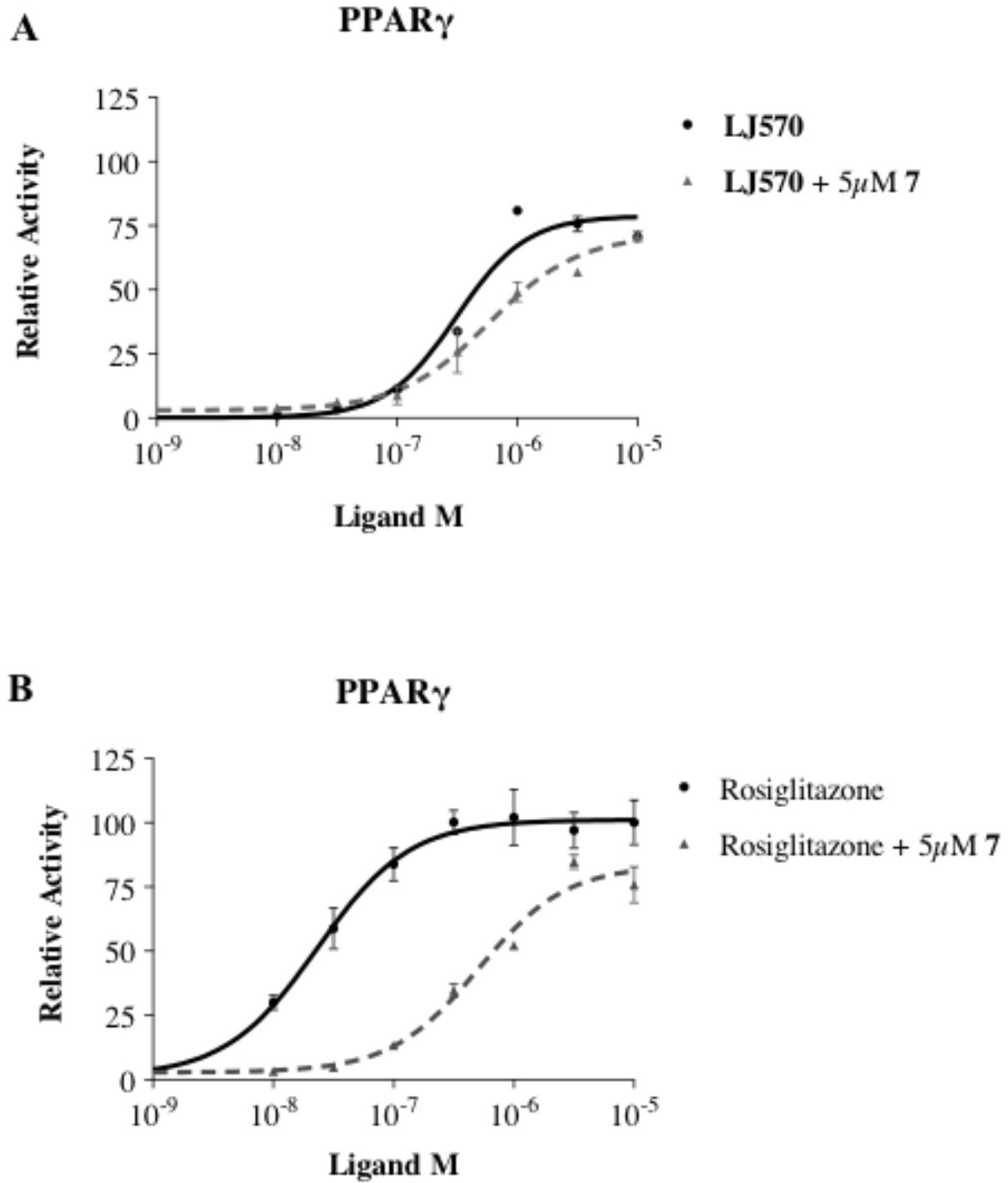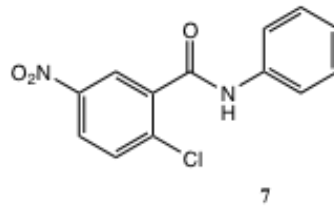
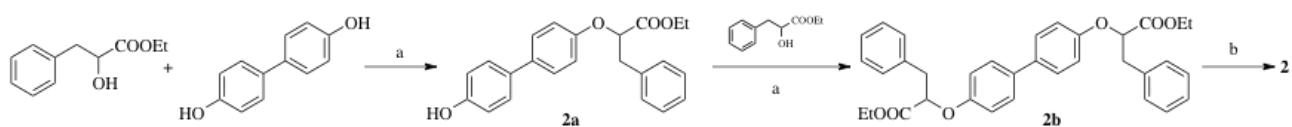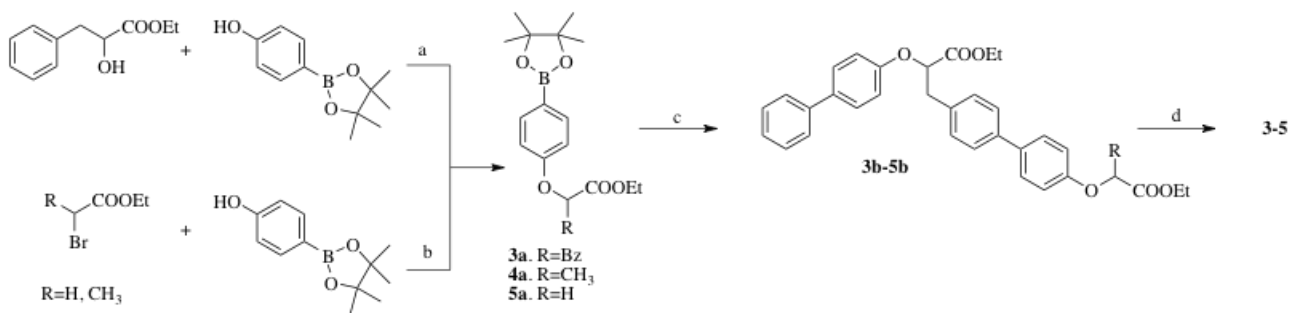**Figure 7.**
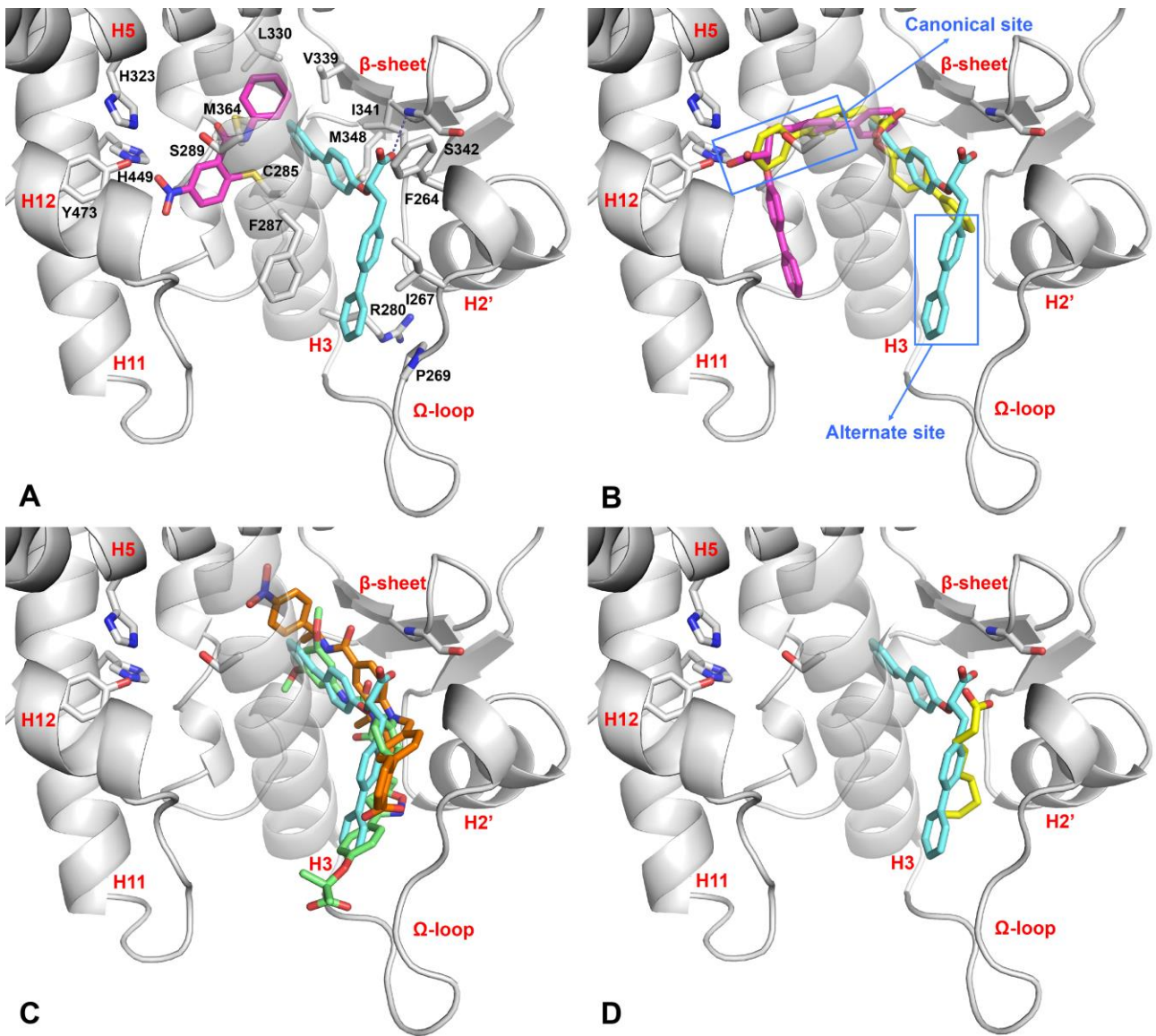
Figure 8.
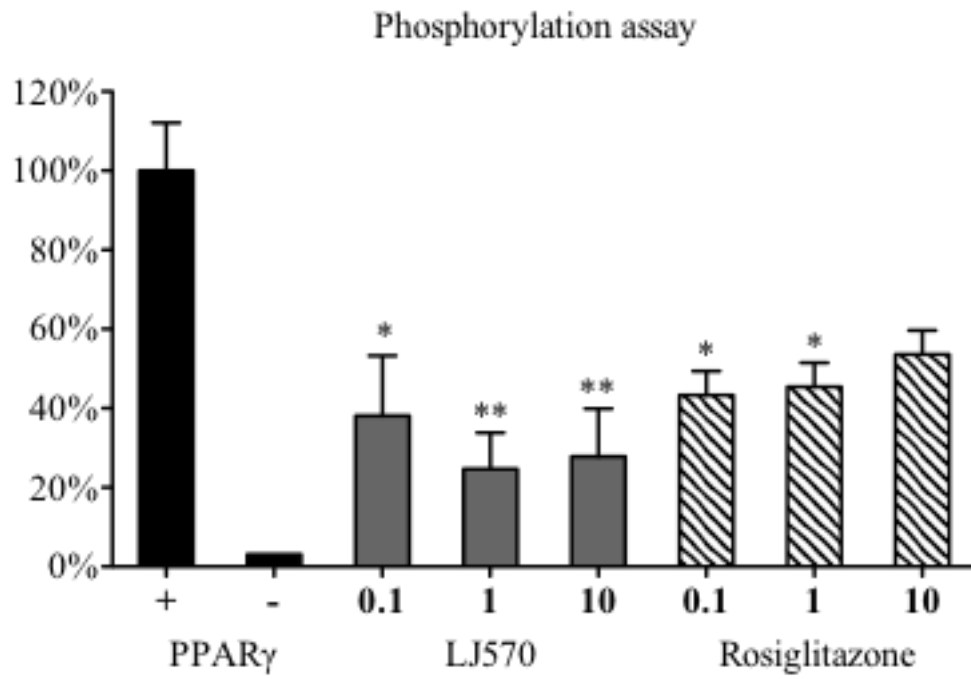
Figure 9.

Figure 10.
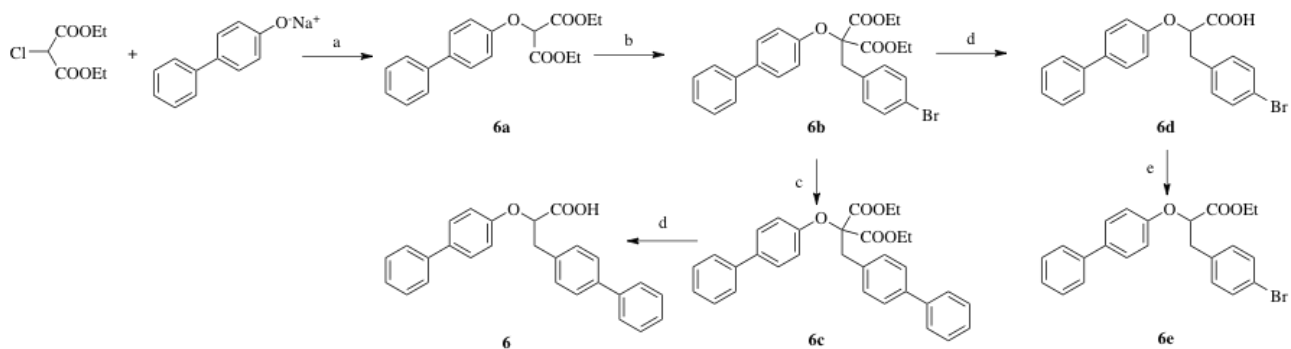
Scheme 1. Synthesis of PPAR agonist **2**.

a) DIAD, PPh₃, anhydrous THF, room temperature, N₂; b) THF/1 N NaOH (1:1), room temperature.
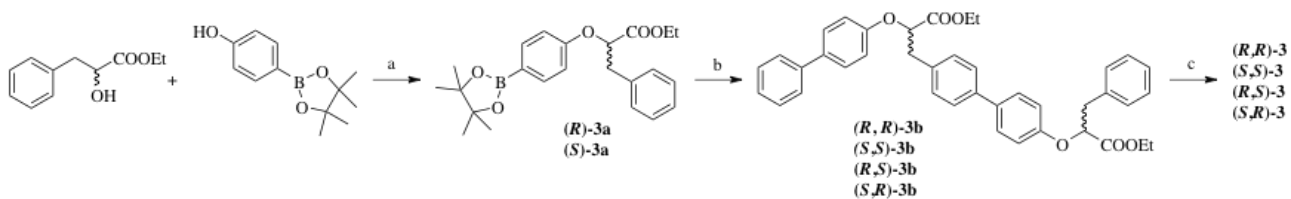
Scheme 2. Synthesis of PPAR agonists **3-5**.

a) DIAD, PPh$_3$, anhydrous THF, room temperature, N$_2$; b) Cs$_2$CO$_3$, anhydrous THF, reflux, N$_2$; c) **6e** (see scheme 3), Cs$_2$CO$_3$, anhydrous toluene, Pd(PPh$_3$)$_4$, 95 °C, N$_2$; d) THF/1 N NaOH (1:1), room temperature.

Scheme 3. Synthesis of PPAR agonist **6**.

a) acetone, reflux; b) NaH, anhydrous DMF, 4-bromo-benzylbromide, 55 °C; c) phenylboronic acid, Cs_2CO_3, anhydrous toluene, $Pd(PPh_3)_4$, 95 °C, N_2; d) 95% EtOH, 1 N NaOH, reflux; e) 95% EtOH, H_2SO_4, reflux.

Scheme 4. Synthesis of the stereoisomers of PPAR agonist **3**.

a) DIAD, PPh_3, anhydrous THF, room temperature, N_2; b) (R)- or (S)-**6g** (see scheme 5), Cs_2CO_3, anhydrous toluene, $Pd(PPh_3)_4$, 95 °C, N_2; c) THF/1 N NaOH (1:1), room temperature.

Scheme 5. Synthesis of the enantiomers of PPAR agonist **6**.
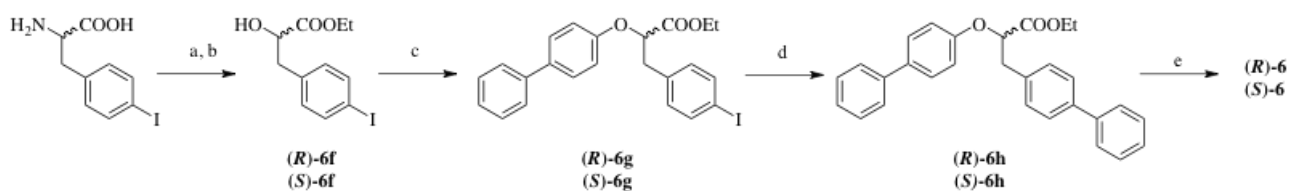
a) acetic acid, 1 N HCl, NaNO$_2$, room temperature; b) abs. EtOH, H$_2$SO$_4$, reflux; c) 4-phenyl-phenol, DIAD, PPh$_3$, anhydrous THF, room temperature, N$_2$; d) phenylboronic acid, Cs$_2$CO$_3$, anhydrous toluene, Pd(PPh$_3$)$_4$, 95 °C, N$_2$; e) THF/1 N NaOH (1:1), room temperature.

Table of Contents graphic

Identification of the First PPARα/γ Dual Agonist Able to Bind to Canonical and Alternate Sites of PPARγ and to Inhibit its Cdk5-Mediated Phosphorylation

Antonio Laghezza, Luca Piemontese, Carmen Cerchia, Roberta Montanari, Davide Capelli, Marco Giudici, Maurizio Crestani, Paolo Tortorella, Franck Peiretti, Giorgio Pochetti, Antonio Lavecchia, Fulvio Loiodice*